Common Capacitor Multiphase LLC Converter With Passive Current Sharing Ability

Hongliang Wang, *Senior Member, IEEE*, Yang Chen, *Student Member, IEEE*, Yajie Qiu, Peng Fang, Yan Zhang, Laili Wang, Yan-Fei Liu, *Fellow, IEEE*, Jahangir Afsharian, and Zhihua (Alex) Yang

***Abstract*—In high-power applications, parallel operation is required to improve both efficiency and reliability. In an LLC converter, it is difficult to achieve parallel operation due to the gain sensitivity to component tolerance. This paper proposes a new structure of a common resonant capacitor for a multiphase LLC converter, which can achieve very good current-sharing performance with no additional components or control. To evaluate the current-sharing performance, a new first harmonic approximation (FHA) model is built in this paper to analyze the LLC converter with coupled resonant tanks. Both FHA analysis and powersim (PSIM) simulation results demonstrate the load-sharing improvement of the proposed common capacitor LLC resonant converter over the conventional two-phase LLC converter. The current-sharing performance from the FHA analysis and the PSIM simulation are compared, and the error of the FHA analysis is evaluated and explained. A 600 W two-phase LLC converter prototype based on the proposed method is also built to verify the feasibility. Excellent current-sharing performance (6% resonant current sharing error at a wide load range) has been achieved.**

***Index Terms*—Current-sharing error, multiphase LLC, resonant converter.**

I. Introduction

RESONANT converter is attractive for isolated dc/dc applications, such as flat-panel displays, laptop adapters, servers, etc., because of its attractive features: smooth waveforms, high efficiency, and high power density. LLC resonant converter has been widely used due to the high efficiency as a result of the zero voltage switching for the primary-side MOSFET and zero current switching for the secondary-side diodes [1]–[6]. Other resonant converters, such as LCC [7]–[10] and LCLC [11]–[15], are also used for industry applications. For the resonant converter used in high power applications, high current stress on the power devices may reduce both efficiency and reliability. Multiphase parallel technique can solve this problem by reducing the current stress in each phase [16]–[19]. However, due to the tolerance of resonant components, the resonant frequency of each individual LLC phase will be different, thus the output currents will be different [20]–[22]. It is observed that a small component tolerance (e.g., 5%) can cause significant current imbalance among phases, and thus degradation of the benefits achieved by the parallel technique. Therefore, current-sharing strategy is mandatory in a multiphase LLC converter.

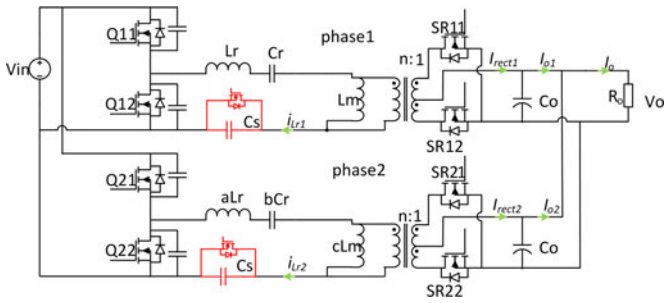

Fig. 1. Switch-controlled capacitor multiphase LLC converter.

Three types of methods have been used to achieve current sharing for multiphase LLC converters [23]–[30]. The first method is based on current loop and frequency control. As a commonly used regulating measure, changing the switching frequency for each phase according to the sensed current will achieve very accurate current-sharing performance. However, the drawback is also obvious in that the method requires two-loop control and additional sensing circuits, which makes the overall system complicated. More important, the switching frequencies of the multiphases are different, so that the overall output voltage ripple has beat frequency components. Thus, the output voltage is prone to either slow regulation or potential stability issue.

Based on same switching frequency, there are two types of methods: the active method and the passive method. The active method uses current-sensing circuits to acquire the current information of each phase and adjusts the voltage gain of different phases by adjusting the equivalent capacitor [23]–[25], inductor [26], phase angle [27], [28], etc.

The circuit diagram with a switch-controlled capacitor is shown in Fig. 1. The circuit diagram with a linearly controlled inductor is shown in Fig. 2, where the value of the resonant inductor is controlled by an additional dc bias winding. Parameters *a, b,* and *c* indicate the tolerances between the two phases. Fig. 3 shows the circuit diagram proposed in [27] and [28]. The three

Manuscript received July 10, 2016; revised November 9, 2016; accepted January 25, 2017. Date of publication January 27, 2017; date of current version October 6, 2017. Recommended for publication by Associate Editor T. Qian.

H. Wang, Y. Chen, Y. Qiu, P. Fang, Y. Zhang, L. Wang and Y.-F. Liu are with the Department of Electrical and Computer Engineering, Queen's University, Kingston, ON K7L 3N6 Canada (e-mail: hongliang.wang@queensu.ca; yang.chen@queensu.ca; yajie.qiu@queensu.ca; p.fang@queensu.ca; yan.zhang@queensu.ca; l.l.wang@queensu.ca; yanfei.liu@queensu.ca).

J. Afsharian and Z. (Alex) Yang are with the Murata Power Solutions, Toronto ON L3R 0J3 Canada (e-mail: jafsharian@murata.com; ZYang@murata.com).

Color versions of one or more of the figures in this paper are available online at http://ieeexplore.ieee.org.

Digital Object Identifier 10.1109/TPEL.2017.2661066

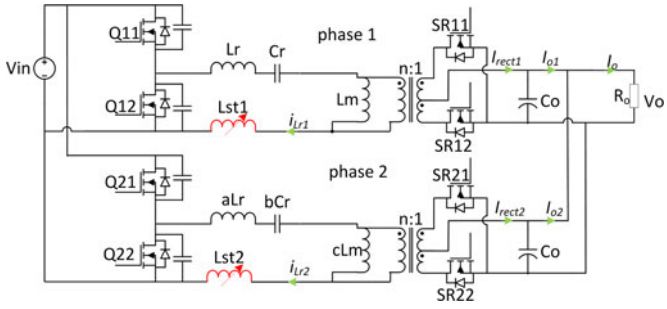

Fig. 2. Linearly controlled inductor multiphase LLC converter.

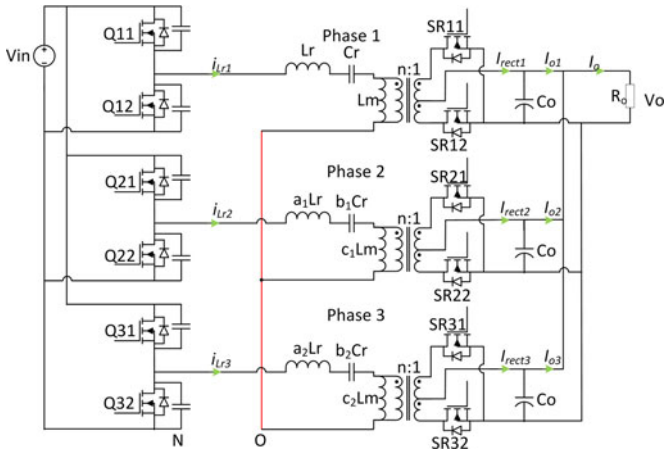

Fig. 3. Three-phase LLC converter with phase shift control.

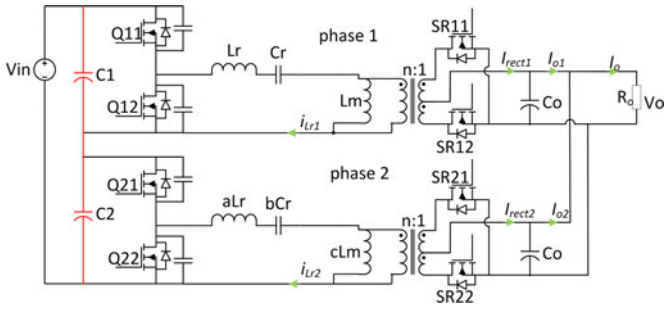

Fig. 4. Series dc-capacitor multiphase LLC converter.

phases have approximately 120° phase angle shift from each other. The resonant components' tolerances are compensated by adjusting the phase shift between the three phases. Good load-sharing performance can be achieved with these methods. However, these methods suffer from high cost, complex control, and nonexcellent dynamic performance caused by the sensing circuit and control loop.

The dc voltage self-balanced method based on series input capacitors is a well-known passive method [29], [30], whose circuit diagram is shown in Fig. 4. Ideally, for two-phase, the two input dc capacitor voltage is the same, and equal to half of the input bus voltage. If the load power is not shared, the midpoint voltage will change based on the output power of each phase. With this method, the system is supposed to have good load current sharing performance. The analysis shows that around 30% current-sharing error can be achieved under +10% tolerance of the resonant inductor, which is not very good. In addition, this method is not suitable for modularization design in system level, as the input voltage for each phase is reduced with the increase in module number. Furthermore, the gate drive circuit for the top phase is complicated.

Therefore, the existing technologies cannot provide cost effective, flexible current sharing technologies for multiphase LLC resonant converters. Recently, the authors have proposed to use passive common inductor technology for the multiphase LLC converter [31], [32]. The resonant inductor of each phase is connected together, such that the common inductor would extract the current information of each phase, and then distribute equally. This concept could also be extended to a common capacitor structure.

In this paper, a common capacitor multiphase LLC resonant converter is proposed [33]. With this method, the resonant capacitor in each LLC phase is connected in parallel to achieve automatic load sharing. Analysis result shows that the load current of each phase can be automatically shared. This technology is simple, so no additional components or control technique is needed. It can be expanded to any number of phases. This paper is organized as follows. Current-sharing analysis of the conventional multiphase LLC resonant converter is given in Section II. Section III discusses the current-sharing analysis of the proposed common capacitor multiphase LLC resonant converter. The simulation results are provided in Section IV. Section V demonstrates the experiment results of a two-phase 600 W prototype between both the conventional method and the proposed method. The paper is concluded in Section VI.

II. Load Current Distribution Analysis of the Conventional Multiphase LLC Converter

With the conventional multiphase LLC structure, resonant component tolerance will cause severe load current imbalance, and degrade the performance of the parallel structure. From the previous research, 5% tolerance on the resonant components would cause separate load—one phase provides all load power, while other phases provide no power. In this section, an improved method will be used to analyze the current-sharing performance. The method can be applied to other type of parallel resonant converter. Section II-A provides the definitions of the parameters, and Section II-B analyzes the current-sharing performance of the direct parallel connection of two LLC converters (conventional two-phase structure).

A. Conventional Two-Phase LLC Resonant Converter

Fig. 5 shows a conventional input-parallel-output-parallel two-phase LLC converter. Q11 and Q12, Q21 and Q22 are the primary half-bridge (HB) switches of phase #1 and phase #2, respectively. Q11, Q21 have same signal, and Q12, Q22 have same signal. SR11 and SR12, SR21 and SR22 are the synchronous rectifiers (SR) on the secondary side of two phases.

L_{r1}, C_{r1}, and L_{m1} are the series resonant inductor, series resonant capacitor, and magnetizing inductor of phase #1. L_{r2}, C_{r2}, and L_{m2} are the series resonant inductor, series resonant capacitor, magnetizing inductor of phase #2. n is

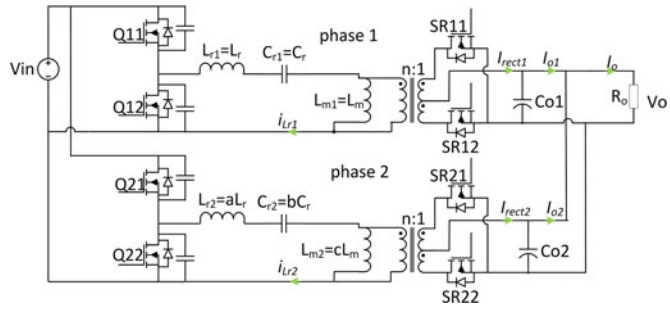

Fig. 5. Conventional two-phase LLLLC resonant converter.

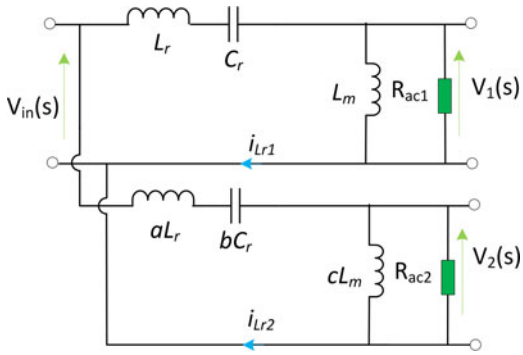

Fig. 6. FHA equivalent circuit of the conventional two-phase LLC resonant converter.

transformer turn ratio. i_{Lr1}, i_{Lr2}, I_{rect1}, I_{rect2}, I_{o1}, I_{o2}, C_{o1}, and C_{o2} are the resonant current, rectifier current, load current, output capacitor of two phases. I_o is the total load current.

Parameters a, b, and c indicate that the resonant parameters for the two phases are different. The resonant tank values of the two phases are

$$\begin{cases} L_{r1} = L_r, & L_{r2} = aL_r \\ C_{r1} = C_r, & C_{r2} = bC_r \\ L_{m1} = L_m, & L_{m2} = cL_m \end{cases}. \tag{1}$$

V_o, P_o, R_o are the output voltage, total output power, and total load resistor of two phases. The load resistor can be expressed as

$$R_o = \frac{{V_o}^2}{P_o}. \tag{2}$$

In the steady-state, each phase will generate part of the total power. P_{o1} is generated by phase #1 and P_{o2} is generated by phase #2

$$P_o = P_{o1} + P_{o2}. \tag{3}$$

The equivalent load resistors R_{o1} and R_{o2} of each phase can be described as

$$\begin{cases} R_{o1} = \frac{{V_o}^2}{P_{o1}} \\ R_{o2} = \frac{{V_o}^2}{P_{o2}} \end{cases}. \tag{4}$$

Define k as the load factor—the proportion of load power generated by phase #1, then P_{o1} and P_{o2} can be expressed as

$$P_{o1} = kP_o \tag{5}$$

$$P_{o2} = (1-k)P_o. \tag{6}$$

Combining (4), (5), and (6) gives

$$\begin{bmatrix} R_{o1} & R_{o2} \end{bmatrix} = \begin{cases} \begin{bmatrix} \infty & R_o \end{bmatrix} & k = 0 \\ \begin{bmatrix} R_o \big/ k & R_o \big/ 1-k \end{bmatrix} & k \in (0,1) \\ \begin{bmatrix} R_o & \infty \end{bmatrix} & k = 1 \end{cases}. \tag{7}$$

When $k = 0$, phase #1 will output no power. Equivalently the load resistor R_{o1} is infinite. Similarly R_{o2} is infinite when $k = 1$. When k is between 0 and 1, then each phase outputs part of the total power.

B. Load Current Distribution Analysis Based on FHA

Several methods have been proposed to analyze the current-sharing performance of the multiphase LLC converter with first harmonic approximation (FHA) equivalent circuit. The existing methods assume that the reflected ac voltage of each phase has same magnitude and same phase angle [22], [34], [35]. However, this assumption is not strictly correct. The output side of each phase is connected together; thus, the magnitude of the reflected ac voltage should have the same magnitude. The phase angle of these reflected ac voltage, however, should be different among different phases, because 1) the component tolerance will create a different phase angle on the resonant current, and 2) the phase of the reflected ac voltage depends on the phase of the resonant current.

Another drawback of the existing analytical method is that the calculation process will require the value of the series resonant frequency of each phase; thus, the method can only be used for decoupled resonant tanks. If the resonant tanks of different phases are coupled, the resonant frequency information of each phase cannot be extracted, and the existing method will be invalid.

A new model is proposed for the two-phase LLC resonant converter [36]. In this paper, the model is used to analyze the current-sharing performance of the proposed common capacitor LLC converter. It is also expanded to multiphase condition. A brief summary of the model is provided here. The key point of the model is that the reflected ac voltage of each phase has same magnitude but different phase angles, due to the tolerance of the resonant components. The new model can be used to analyze the multiphase resonant converter with both coupled and decoupled resonant tanks. The FHA equivalent circuit is shown in Fig. 6.

$V_1(s)$ and $V_2(s)$ are the reflected ac voltages on the primary side of transformer for these two phases.

The primary-side equivalent ac resistors R_{ac1} and R_{ac2} can be calculated as

$$\begin{cases} R_{\mathrm{ac1}} = \frac{8n^2}{\pi^2} R_{o1} \\ R_{\mathrm{ac2}} = \frac{8n^2}{\pi^2} R_{o2} \end{cases}. \tag{8}$$

Combing (7) and (8) gives

$$\begin{bmatrix} R_{\mathrm{ac1}} & R_{\mathrm{ac2}} \end{bmatrix} = \begin{cases} \begin{bmatrix} \infty & \frac{8n^2}{\pi^2}R_o \end{bmatrix} & k=0 \\ \begin{bmatrix} \frac{8n^2R_o}{\pi^2 k} & \frac{8n^2R_o}{\pi^2(1-k)} \end{bmatrix} & k\in(0,1) \\ \begin{bmatrix} \frac{8n^2}{\pi^2}R_o & \infty \end{bmatrix} & k=1 \end{cases}. \quad (9)$$

As the two phases are connected in parallel at both input side and output side, thus in steady-state operation, the voltage gain of the two phases is the same. The magnitude of ac voltage $V_1(s)$ and $V_2(s)$ is the same. The relationship is shown as

$$|V_1(s)| = |V_2(s)|. \quad (10)$$

According to the FHA model shown in Fig. 6, the transfer function of $V_1(s)$, $V_2(s)$ can be calculated as

$$\begin{cases} V_1(s) = \frac{R_{\mathrm{ac1}}//sL_m}{R_{\mathrm{ac1}}//sL_m+sL_r+1/sC_r}V_{\mathrm{in}}(s) \\ V_2(s) = \frac{R_{\mathrm{ac2}}//scL_m}{R_{\mathrm{ac2}}//scL_m+saL_r+1/sbC_r}V_{\mathrm{in}}(s) \end{cases}. \quad (11)$$

Manipulating (9), (10), and (11), the load factor k can be calculated by

$$Ak^2+Bk+C=0. \quad (12)$$

For the conventional two-phase LLC converter, the parameters *A, B, C* are expressed as

$$\begin{cases} A = \omega^2(1-b^2)c^2{L_m}^2 - \omega^4(2ab-2b^2)c^2L_r{L_m}^2C_r \\ \quad +\omega^6(a^2-1)b^2c^2{L_r}^2{L_m}^2{C_r}^2 \\ B = -2\omega^2c^2{L_m}^2 + 4\omega^4abc^2L_r{L_m}^2C_r \\ \quad -2\omega^6a^2b^2c^2{L_r}^2{L_m}^2{C_r}^2 \\ C = \omega^2c^2{L_m}^2 - 2\omega^4abc^2L_r{L_m}^2C_r + \omega^6a^2b^2c^2{L_r}^2{L_m}^2{C_r}^2 \\ \quad +(1-b^2c^2){R_{\mathrm{ac}}}^2 - \omega^2[(2ab-2b^2c^2)L_r \\ \quad +(2bc-2b^2c^2)L_m]C_r{R_{\mathrm{ac}}}^2 + \omega^4(ab-bc)[(ab+bc){L_r}^2 \\ \quad +2bcL_rL_m]{C_r}^2{R_{\mathrm{ac}}}^2 \\ \omega = 2\pi f_s \end{cases} \quad (13)$$

in which ω is the angular frequency of the primary HB switches; *a*, *b,* and *c* are the tolerances between the two phases; and R_{ac} is the total equivalent ac load resistor.

The value of load factor *k* can then be derived with

$$k = \begin{cases} -\frac{C}{B} & A=0,\ B\neq 0 \\ \frac{-B\pm\sqrt{B^2-4AC}}{2A} & A\neq 0,\ \sqrt{B^2-4AC}\geq 0 \end{cases}$$

and $k\in[0,1]$. (14)

The value of *k* is valid when *k* is between 0 and 1. $k=0.5$ means the load power can be equally shared by two phases. $k=0$ and $k=1$ mean only one phase provides all the power and the other phase does not provide any power. Conditions $k<0$ and $k>1$ are not valid answers.

To evaluate the current-sharing performance, the load current sharing error σ_{load} is

$$\sigma_{\mathrm{load}} = \mathrm{abs}\left[\frac{I_{01}-I_{02}}{I_{01}+I_{02}}\right] = \mathrm{abs}\,(1-2k),\ k\in[0,1] \quad (15)$$

where I_{o1} and I_{o2} are the dc output current value for phase #1 and phase #2. According to the physical meaning of load factor *k*, it can be inferred that $\sigma_{\mathrm{load}}=0$ means the load power being equally shared, while $\sigma_{\mathrm{load}}=1$ means only one phase provides all the power.

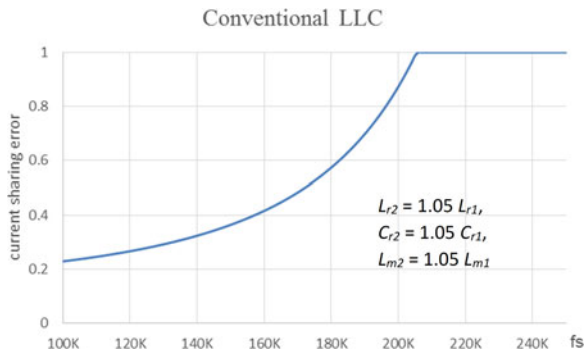

Fig. 7. Relationship between current-sharing error and switching frequency for the conventional structure.

TABLE I
NOMINAL PARAMETER VALUE

Input voltage range	350–400 V
Resonant inductor L_r	29 μH
Resonant capacitor C_r	12 nF
Magnetizing inductor L_m	95 μH
Transformer ratio *n*	20
Resonant frequency f_r	270 kHz
Output voltage V_o	12 V (rated voltage)
Total Output load P_o	One phase power 300 W (25 A)
	Two phase power 600 W (50 A)

Fig. 7 shows the curve of current-sharing error changing with switching frequency for the conventional two-phase LLC converter. The resonant parameters from Table I are used. The *a, b,* and *c* values are 1.05, 1.05, and 1.05, which will be proved as the worst case in the later part. Another cases have similar trend. As can be observed in the figure, for the conventional structure, the current-sharing error increases with switching frequency. When the switching frequency is close to the resonant frequency of 270 kHz, the current-sharing error is 100%, so it means only one phase provides all the load power while the other phase provides no power.

As a supplement, the resonant current sharing error $\sigma_{\mathrm{resonant}}$ is

$$\sigma_{\mathrm{resonant}} = \mathrm{abs}\left[\frac{\mathrm{rms}(i_{\mathrm{Lr1}})-\mathrm{rms}(i_{\mathrm{Lr2}})}{\mathrm{rms}(i_{\mathrm{Lr1}})+\mathrm{rms}(i_{\mathrm{Lr2}})}\right] \quad (16)$$

where $\mathrm{rms}(i_{\mathrm{Lr1}})$, $\mathrm{rms}(i_{\mathrm{Lr2}})$ are the root mean square (rms) value of resonant current i_{Lr1} and i_{Lr2}.

When *N* ($N>2$) phases are connected in parallel, the load current sharing error and resonant current sharing error for a certain phase can be shown as

$$\sigma_{\mathrm{resonant}} = \mathrm{abs}\left[\frac{\mathrm{rms}(i_{\mathrm{Lr1}})-\mathrm{rms}(i_{\mathrm{Lr2}})}{\mathrm{rms}(i_{\mathrm{Lr1}})+\mathrm{rms}(i_{\mathrm{Lr2}})}\right] \quad (17)$$

where *N* is total phase count; $\mathrm{rms}(i_{\mathrm{Lrj}})$ and I_{oj} are, respectively, the resonant current rms value and output current dc value of the *j*th phase.

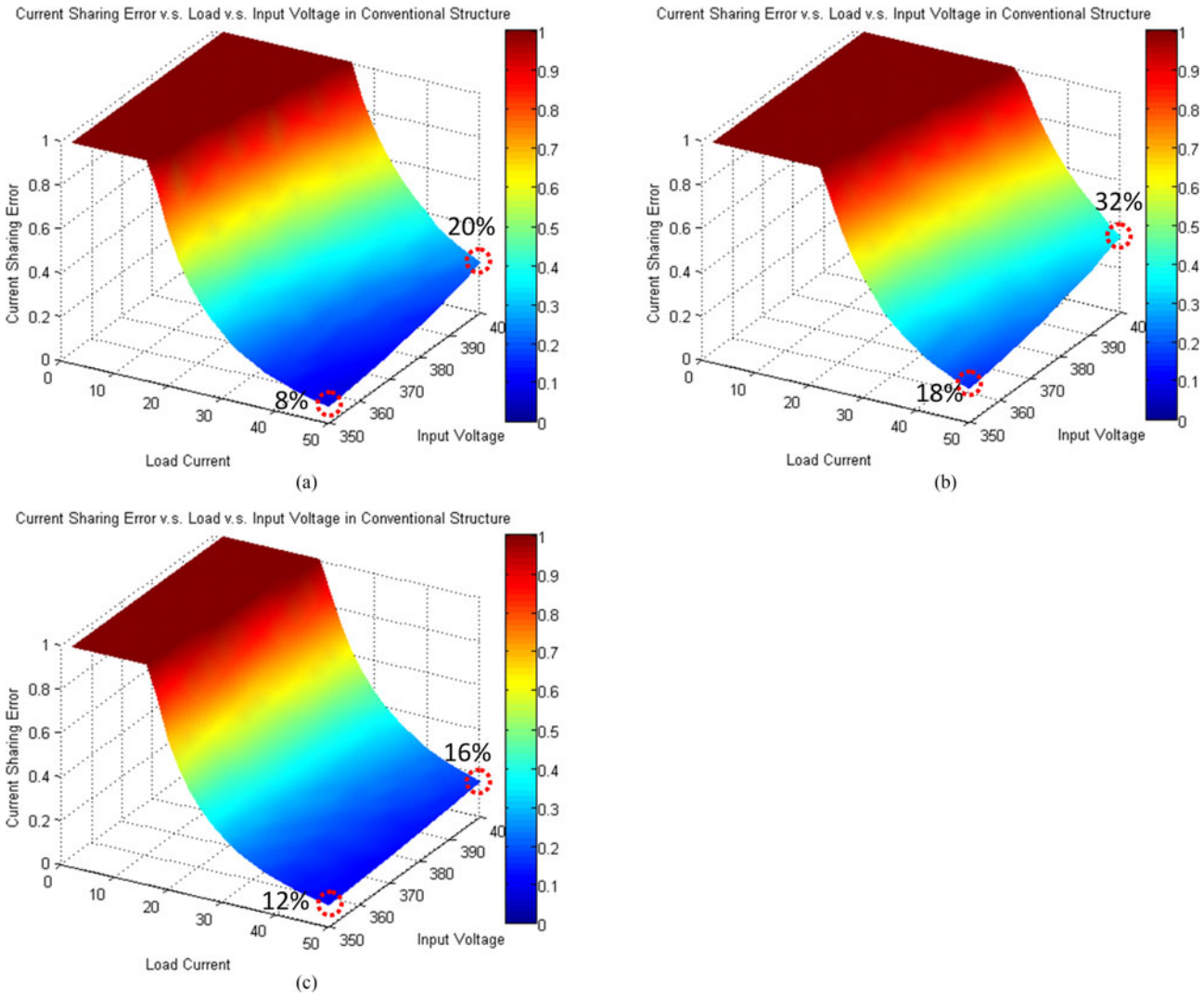

Fig. 8. Current-sharing error of the conventional two-phase LLC converter with +5% tolerance of single parameter: (a) +5% L_r parameter tolerance ($a = 1.05$, $b = 1$, $c = 1$); (b) +5% L_r parameter tolerance ($a = 1$, $b = 1.05$, $c = 1$); and (c) +5% L_r parameter tolerance ($a = 1$, $b = 1$, $c = 1.05$).

C. Current-Sharing Performance in Different Input and Load Conditions

To demonstrate the load-sharing performance of the conventional two-phase LLC converter in different input and load conditions, the differences of the two-phase load currents are calculated with the FHA method based on the set of parameters shown in Table I designed by the existing method [37]. The parameters shown in Table I are assigned to phase #1 as the reference, while parameters of phase #2 will have ±5% tolerances, which is a common value for off-the-shelf capacitors and inductors.

Fig. 8 shows load current sharing error of the two-phase LLC converter in the conventional structure under different input voltage and load current conditions.

Only the tolerance of one component is considered. The input voltage is from 350 to 400 V on *x*-axis. The total load current range for two phases is from 0 to 50 A (600 W) shown on *y*-axis. *Z*-axis shows the load current sharing error σ_{load} between the two phases.

In Fig. 8(a), +5% tolerance on L_r only is considered, which means L_{r2} is 5% larger than L_{r1}, while C_{r1} and L_{m1} are the same with C_{r2} and L_{m2} ($a = 1.05$, $b = 1$, $c = 1$). It is observed that only one phase provides power when the total load is below 25 A. At 400 V input and full load 50 A, the load difference of the two phases is 20%—meaning one phase provides 30 A (25 A +20%), while the other provides 20 A (25 A –20%).

In Fig. 8(b), +5% tolerance on C_r only ($a = 1$, $b = 1.05$, $c = 1$) is considered. C_{r2} is 5% larger than C_{r1}, while L_{r1} and L_{m1} are the same with L_{r2} and L_{m2}. At 400 V input and full load 50 A condition, the load difference of the two phases is 32%, which means one phase provides 33 A (25 A +32%), while the other provides 17 A (25 A –32%).

Similarly in Fig. 8(c), +5% tolerance on L_m only ($a = 1$, $b = 1$, $c = 1.05$) is considered. At 400 V input and full load 50 A condition, the load difference of the two phases is 16%, which means one phase provides 29 A (25 A +16%), while the other provides 21 A (25 A –16%).

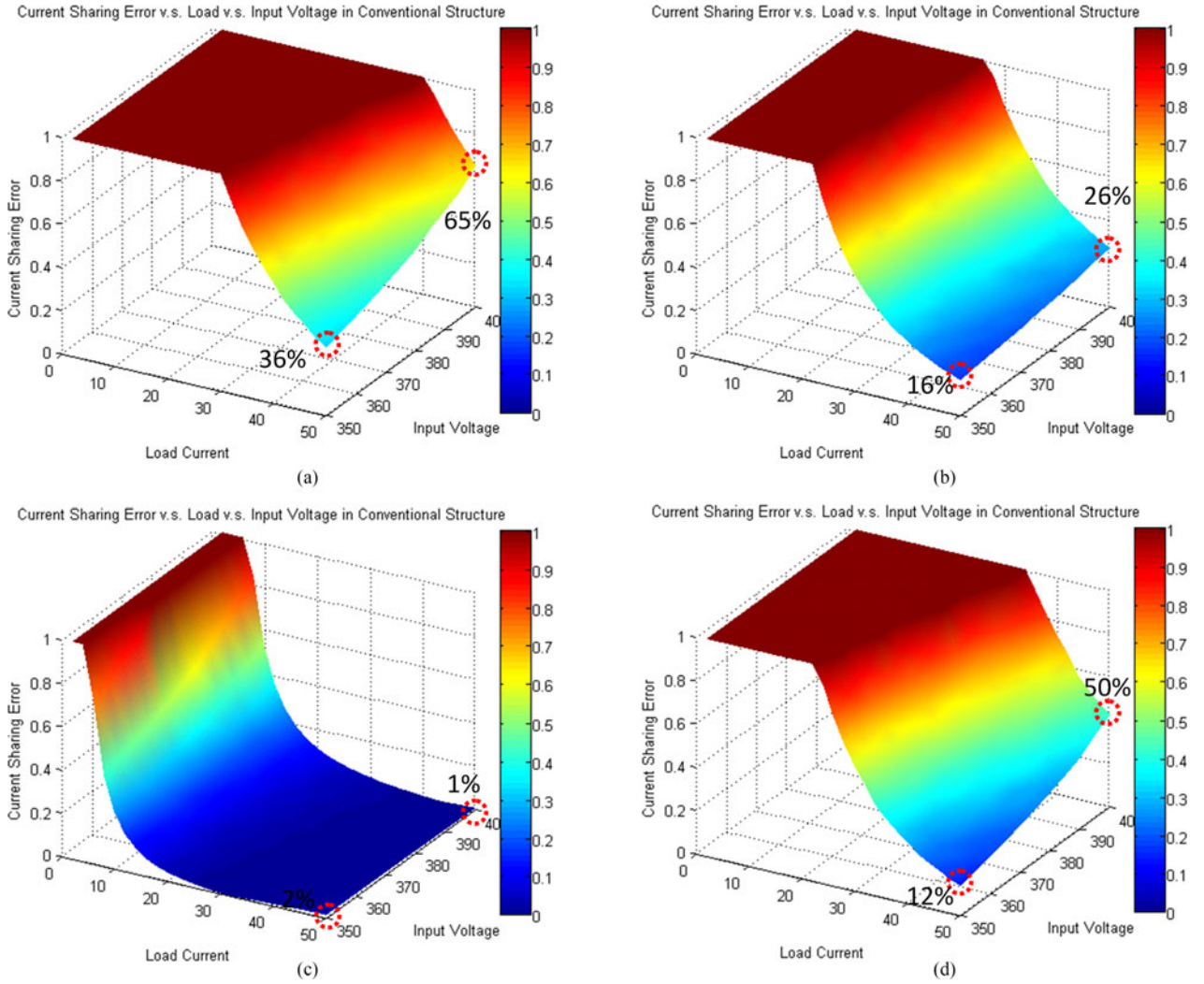

Fig. 9. Current-sharing error of the conventional two-phase LLC converter with +5% tolerance of three parameters: (a) +5% L_r +5% C_r +5% L_m tolerance ($a = 1.05$, $b = 1.05$, $c = 1.05$); (b) –5% L_r +5% C_r +5% L_m tolerance ($a = 0.95$, $b = 1.05$, $c = 1.05$); (c) +5% L_r –5% C_r +5% L_m tolerance ($a = 1.05$, $b = 0.95$, $c = 1.05$); and (d) +5% L_r +5% C_r –5% L_m tolerance ($a = 1.05$, $b = 1.05$, $c = 0.95$).

For –5% case, the load-sharing error is basically the same but opposite distribution between the two phases. For example, at 400 V input and 50 A total load, if L_{r2} is 5% larger than L_{r1} ($a = 1.05$), phase #2 will provide 20 A and phase #1 will provide 30 A; thus, the current-sharing error is 20% [0.2 shown in Fig. 8(a)]. While if L_{r2} is 5% smaller than L_{r1} ($a = 0.95$), then phase #1 will provide 20 A of total load and phase #2 will provide 30 A, and the current-sharing error is still 20%.

From Fig. 8, it is observed that the load current sharing error increases with the increase in input voltage. For the conventional two-phase LLC converter, the current-sharing error increases with the increase in switching frequency. According to frequency modulation, at higher input voltage, the switching frequency is higher. Thus, equivalently, the current-sharing error increases with the increase in input voltage. This characteristic, however, is not favorable especially in some applications that require the converter to operate for long time at high voltage, e.g., data center and server power supply operating at rated 400 V. Comparing the current-sharing error in Fig. 8(a)–(c), it could be concluded that the tolerance on C_r has the most significant impact on current sharing of multiphase LLC converters.

Fig. 9 shows load current sharing error σ_{load} of the conventional two-phase LLC converter with 5% tolerances combinations of L_r, C_r, and L_m. Theoretically there are total eight (2^3) possible combinations for L_r C_r, and L_m at ±5% tolerance. Four of the total eight combinations are just equivalent to the rest four types—current-sharing error is the same while current distribution is opposite. For example, tolerance combination +5% on L_r, +5% on C_r, +5% on L_m ($a = 1.05$, $b = 1.05$, $c = 1.05$) is equivalent to combination –5% on L_r, –5% on C_r, –5% on L_m ($a = 0.95$, $b = 0.95$, $c = 0.95$); and combination –5% on L_r, +5% on C_r, +5% on L_m ($a = 0.95$, $b = 1.05$, $c = 1.05$) is equivalent to that of +5% on L_r, –5% on C_r, –5% on L_m ($a = 1.05$, $b = 0.95$, $c = 0.95$). Thus, the four types of combination shown in Fig. 9 have covered all possible cases at 5% tolerance level in terms of current-sharing error. In Fig. 9(a), +5% tolerance on L_r, C_r, and L_m as a whole is analyzed, which means L_{r2}, C_{r2}, and L_{m2} are 5% larger than L_{r1}, C_{r1},

and L_{m1}, respectively ($a = 1.05$, $b = 1.05$, $c = 1.05$). No load sharing could be achieved until the total load reaches 40 A. At 400 V input and full load 50 A, the load difference of the two phases is 65%—meaning one phase provides 41 A (25 A +65%), while the other provides 9 A (25 A –65%).

In Fig. 9(b), –5% tolerance on L_r, +5% tolerance on C_r and L_m ($a = 0.95$, $b = 1.05$, $c = 1.05$) is considered. At 400 V input and full load 50 A condition, the load difference of the two phases is 26%, which means one phase provides 31.5 A (25 A +26%), while the other provides 18.5 A (25 A –26%).

Similarly in Fig. 9(c), +5% tolerance on L_r, –5% tolerance on C_r, and +5% tolerance on L_m ($a = 1.05$, $b = 0.95$, $c = 1.05$) is analyzed. The tolerances on L_r and C_r are opposite and counteractive that the resonant frequency of the two phases are the same. This explains why good load sharing can be achieved for wide input voltage and load range. At 400 V input and full load 50 A condition, the current-sharing error of the two phases is close to 0.

In Fig. 9(d), +5% tolerance on L_r and C_r, and –5% tolerance on L_m ($a = 1.05$, $b = 1.05$, $c = 0.95$) is considered. At 400 V input and full load 50 A condition, the load difference of the two phases is 50%, which means one phase provides 37.5 A (25 A +50%), while the other provides 12.5 A (25 A –50%).

From Fig. 9, it can be observed that, for a conventional structure of the two-phase LLC converter, the worst case for current-sharing performance occurs when the tolerance parameters *a, b, c* deviate in the same direction at case +5% on L_r, +5% on C_r, +5% on L_m ($a = 1.05$, $b = 1.05$, $c = 1.05$). The reason could be explained as following. If $L_{r2} > L_{r1}$ or $C_{r2} > C_{r1}$ and $L_{m2} = L_{m1}$, then phase #2 will have lower resonant frequency as compared with phase #1. Assuming same load, at given switching frequency, phase #2 will have lower voltage gain. As both output and input voltages are of same magnitude, the two phases must achieve same voltage gain. This forces phase #1 to provide more power and phase #2 provides less power. If $L_{r2} = L_{r1}$ or $C_{r2} = C_{r1}$ and $L_{m2} > L_{m1}$, phase #2 will have higher inductor ratio, which results in lower voltage gain. Then, phase #1 will provide more power to keep the output voltage same with phase #2. Thus, the worst case is that parameters *a, b, c* deviate in the same direction.

In practice, the worst-case condition will determine the overall performance of the multiphase LLC converter. Specifically, at 400 V and total 50 A load condition, the difference of two phase load current reaches 65% of total load current [see Fig. 9(a)], meaning one phase outputting 41 A and the other phase outputting only 9 A. Thus, for a total 50 A/600 W two-phase LLC converter with the conventional structure, each phase has to be designed with rated 41 A rather than desired 25 A to ensure the safe operation. This will defeat the purpose of parallel connection.

III. Current-Sharing Perfromance of the Common Capacitor Multiphase LLC Converter

As shown in Fig. 5, the two LLC phases in the conventional structure are connected in parallel at both the input side and the output side. Thus, the resonant tank of each phase is completely independent of the other phase. No current information can be exchanged between the phases, and no current sharing can be achieved.

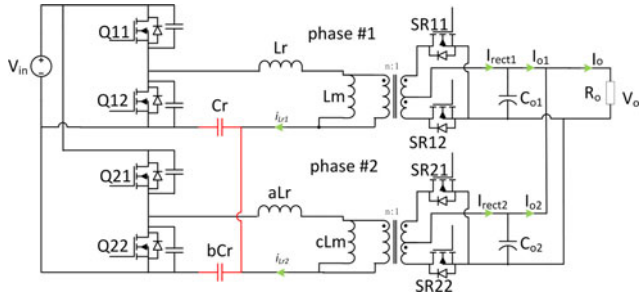

Fig. 10. Common capacitor two-phase LLC resonant converter.

Following this thought, it could be suggested that the current information of each phase must be collected in order to achieve current sharing for multiphases converters. Collecting the current information can be implemented by current-sensing circuit.

In this section, a new multiphase LLC resonant converter is proposed. The resonant capacitors of different phases are connected in parallel to form a common capacitor branch, which will take in the current information of each phase and then redistribute evenly. For simple understanding, a two-phase common capacitor LLC resonant converter will be discussed in this section. Current-sharing performance will be evaluated through the FHA analysis.

A. Common Capacitor Multiphase LLC Converter

Fig. 10 shows the common capacitor two-phase LLC resonant converter. The series resonant capacitors of the two LLC converters are connected together in parallel. The paralleled two resonant capacitors can also be implemented with only one capacitor with value equals to the total capacitance of $(1 + b)_* C_r$. It should be noted that the switch node of Q11/Q12 could be directly connected to the switching node of Q21/Q22, so to utilize the positive temperature coefficient of MOSFETs. However, with this configuration, phase shedding cannot be achieved.

The authors have proposed the passive-impedance-matching concept to explain the current-sharing mechanism from the equivalent circuit point of view [38], [39]. According to the analysis, the common capacitor resonant tank could be decoupled and equivalent to a capacitor plus a resistor for each phase. The equivalent resistor will always be of opposite sign for the two phases. If phase #1 has higher current than phase #2, the equivalent resistor for phase #1 will be positive. And the equivalent resistor of phase #2 will be negative. As a result, the power in phase #1 is reduced, and the power of phase #2 is increased. This intrinsic negative feedback will guarantee good current-sharing performance for the common capacitor multiphase LLC converter.

B. Current-Sharing Analysis of the Two-Phase Common Capacitor LLC Converter

In this paper, FHA is still used to analyze the current-sharing performance. Same as the conventional two-phase LLC

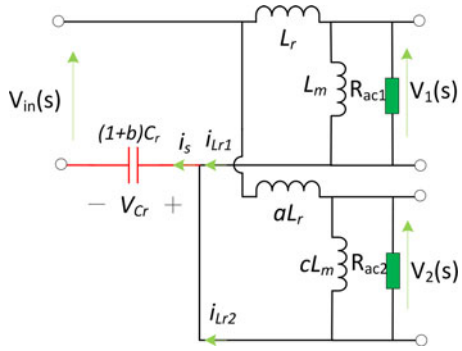

Fig. 11. FHA equivalent circuit of the two-phase common capacitor LLC resonant converter.

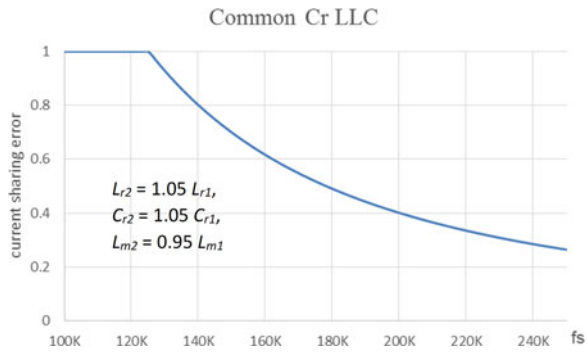

Fig. 12. Relationship between current-sharing error and switching frequency for common capacitor LLC at full load case.

converter, the output power P_o is divided into P_{o1} for phase #1 and P_{o2} for phase #2. And (2)–(10) are still valid in the analysis of the proposed two-phase common capacitor LLC converter.

Fig. 11 shows the FHA circuit of the proposed two-phase common capacitor LLC converter. The total resonant capacitance C_{r_total} is

$$C_{r\_\mathrm{total}} = (1+b)\,C_r. \tag{18}$$

From Fig. 11, the transfer function of ac voltage $V_1(s)$, $V_2(s)$ is

$$\begin{cases} V_1(s) = \frac{R_{\mathrm{ac1}}//sL_m}{R_{\mathrm{ac1}}//sL_m + sL_r}(V_{\mathrm{in}}(s) + V_{\mathrm{Cr}}(s)) \\ V_2(s) = \frac{R_{\mathrm{ac2}}//s(cL_m)}{R_{\mathrm{ac2}}//s(cL_m)+s(aL_r)}(V_{\mathrm{in}}(s) + V_{\mathrm{Cr}}(s)) \end{cases}. \tag{19}$$

The load factor k still complies to the quadratic equation shown in (12), while for the two-phase common capacitor LLC converter, the coefficients *A, B, C* are expressed as

$$\begin{cases} A = \omega^4(a^2-1)c^2{L_r}^2{L_m}^2 \\ B = -2\omega^4a^2c^2{L_r}^2{L_m}^2 \\ C = \omega^4a^2c^2{L_r}^2{L_m}^2 + \omega^2[(a^2-c^2){L_r}^2 \\ \quad +2(ac-c^2)L_rL_m]{R_{\mathrm{ac}}}^2 \\ \omega = 2\pi f_s \end{cases}. \tag{20}$$

Combing (12) and (20), the load factor k can be solved for different input voltage and load conditions for the two-phase common capacitor LLC converter. Accordingly, the load current sharing error σ_{load} and resonant current sharing error $\sigma_{\mathrm{resonant}}$ can be calculated with (15) and (16), respectively. For the multiphase common capacitor LLC converter with more than two phases, the load current sharing error σ_{load} can be calculated with (17).

Fig. 12 shows the curve of current-sharing error changing with switching frequency for the common capacitor two-phase LLC converter. The resonant parameters are from Table I. The *a*, *b,* and *c* values are 1.05, 1.05, and 0.95, which will be proved as the worst case in the later part. Another case has similar trend. Opposite from the result of the conventional structure, the current-sharing error of the common capacitor structure decreases with switching frequency. Thus, when the switching frequency is near the resonant point (270 kHz), the current-sharing performance is better.

C. Current-Sharing Performance in Different Input and Load Conditions

To demonstrate the load current sharing performance of the proposed two-phase common capacitor LLC converter in different input and load conditions, the load current sharing error σ_{load} is calculated with the FHA method based on the set of parameters shown in Table I. The parameters shown in Table I are assigned to phase #1 as the reference, while parameters of phase #2 will have ±5% tolerances.

Fig. 13(a) shows the load current sharing error σ_{load} with +5% tolerance on L_r only ($a = 1.05$, $b = 1$, $c = 1$). Similarly in Fig. 13(b) and (c), +5% tolerance on C_r only ($a = 1$, $b = 1.05$, $c = 1$) and +5% tolerance on L_m only ($a = 1$, $b = 1$, $c = 1.05$) are considered, respectively.

Comparing Fig. 13(a) with Fig. 8(a) and Fig. 13(c) with Fig. 8(c), it can be observed that similar load current sharing performance is achieved for the conventional structure and the proposed common capacitor structure for L_m and L_r tolerance. Comparing Fig. 13(b) with Fig. 8(b), however, the scenario is very different. As is observed in Fig. 13(b), the load current sharing error is zero despite the input and load condition. Thus, with the proposed two-phase common capacitor structure, the impact of C_r tolerance is fully removed. This is understandable as two capacitors are connected in parallel.

Fig. 14 shows load current sharing error σ_{load} of the two-phase common capacitor LLC converter with ±5% tolerances combinations of L_r, C_r, and L_m. As explained in Section II-C, Fig. 14(a)–(d) covers all tolerances combinations at ±5% level. Comparing Fig. 14(a) with (c), the current-sharing performance is the same even though the tolerance on C_r is opposite (L_r and L_m are the same). This verifies the conclusion of Fig. 13(b) that the impact of C_r tolerance is fully removed with the common capacitor structure. Same results can be found in Fig. 14(b) and (d).

It is observed from Fig. 14(a) and (c), the load-sharing error is close to 0 for a wide input and load range. It is observed from Fig. 14(b) and (d), at 400 V input and full load 50 A condition, the load difference of the two phases is 36%, which means one phase provides 34 A (25 A +36%), while the other

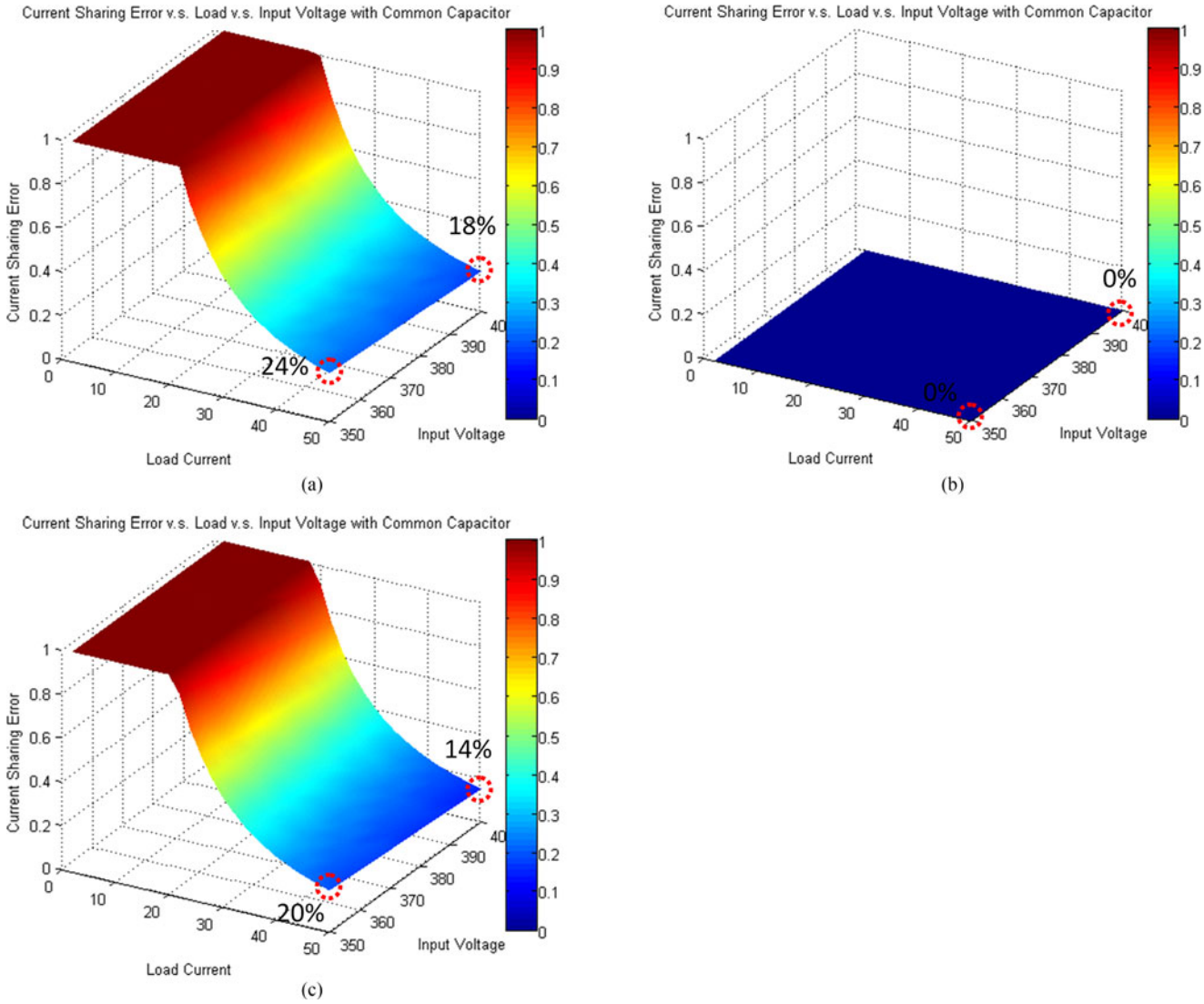

Fig. 13. Current-sharing error of the two-phase common capacitor LLC converter with +5% tolerance of single parameter: (a) +5% L_r parameter tolerance ($a = 1.05, b = 1, c = 1$); (b) +5% L_r parameter tolerance ($a = 1, b = 1.05, c = 1$); and (c) +5% L_r parameter tolerance ($a = 1, b = 1, c = 1.05$).

provides 16 A (25 A –36%). The worst case for current-sharing performance occurs when the tolerance on L_r and the tolerance on L_m deviate in the opposite direction shown in Fig. 14(b) and (d). The reason can be explained as following. According to Fig. 11 and (19), L_r and $(L_m//R_{\rm ac})$ form a voltage divider circuit. Thus, if the tolerance on L_r and the tolerance on L_m deviate in the same direction with same amount (e.g., $a = 1.05$ and $c = 1.05$), then difference between $R_{\rm ac1}$ and $R_{\rm ac2}$ must be around 5% to keep $V_1(\rm s)$ and $V_2(\rm s)$ of same magnitude. On the contrary, if the tolerance on L_r and the tolerance on L_m deviate in the opposite direction (e.g., $a = 1.05$ and $c = 0.95$), then to keep $V_1(\rm s)$ and $V_2(\rm s)$ of same magnitude, the difference of $R_{\rm ac1}$ and $R_{\rm ac2}$ will be at the maximum (>>5%), meaning worst current-sharing performance.

In practice, the worst case will determine the overall performance of the multiphase LLC converter. Specifically, from 350 to 400 V, at total 50 A load condition, the difference of two phase load current reduces from 65% in the conventional structure to 40% in the proposed common capacitor structure [see Fig. 14(b) and (d)]. It should be noted that the current-sharing performance for the common capacitor LLC converter is much better based on the computer simulation and additional analysis provided in the next section. In simulation, the worst current-sharing error of 400 V case is 12%. The assumption of FHA causes the large current-sharing error.

D. Phase Shedding and Interleaving Capability

For parallel operation of the converters, except for the current-sharing ability, features such as phase shedding and interleaving are also desired.

The proposed common capacitor LLC converter could achieve phase shedding. If phase #2 is shut down, all the components in phase #2 will not operate except C_{r2}. It should be noted that the total resonant capacitance for phase #1 will be $C_{r1} + C_{r2}$, if phase #2 is shed. The new resonant frequency

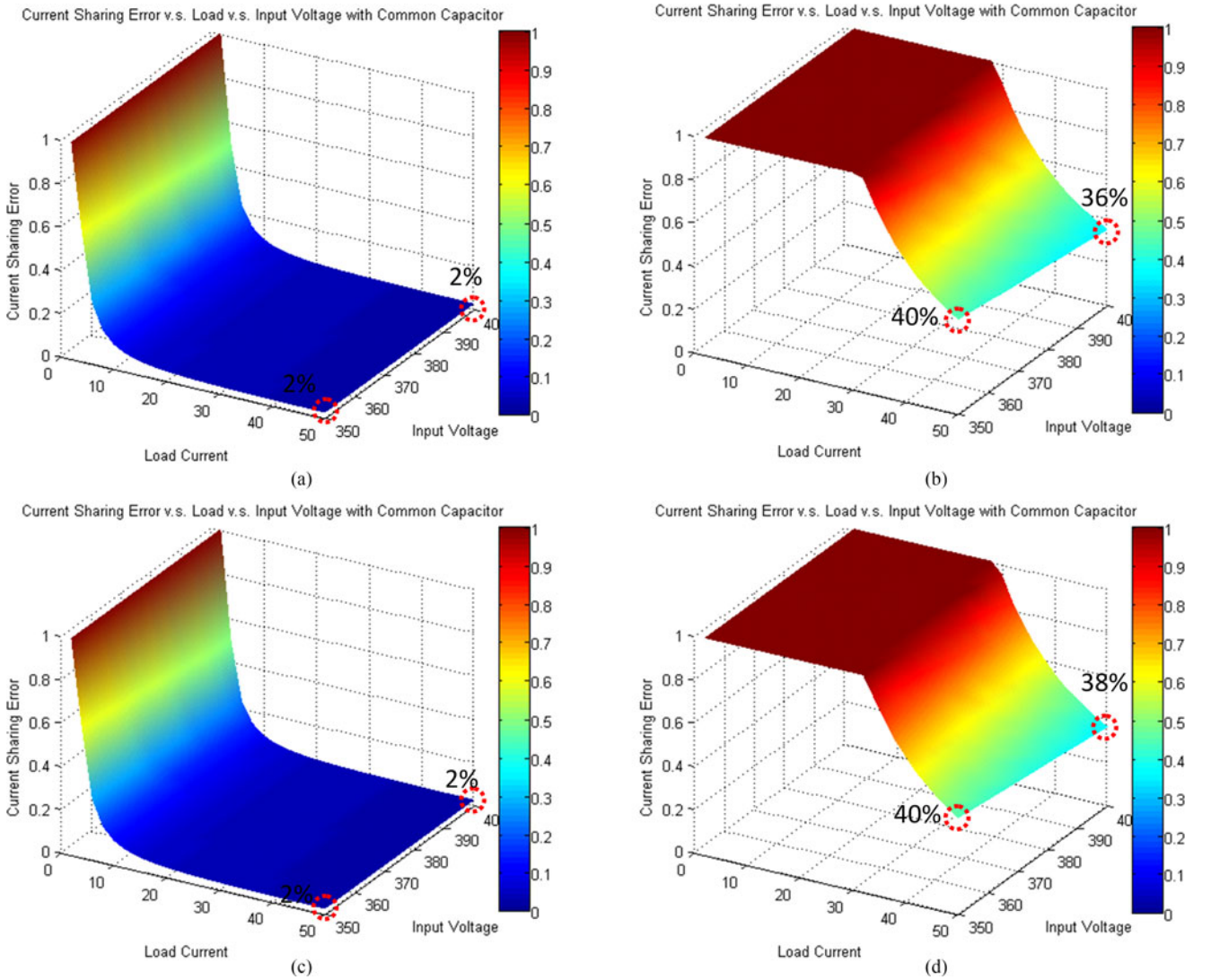

Fig. 14. Current-sharing error of the common capacitor LLC converter with +5% tolerance combination of three parameters: (a) +5% L_r +5% C_r +5% L_m tolerance ($a = 1.05$, $b = 1.05$, $c = 1.05$); (b) –5% L_r +5% C_r +5% L_m tolerance ($a = 0.95$, $b = 1.05$, $c = 1.05$); (c) +5% L_r –5% C_r +5% L_m tolerance ($a = 1.05$, $b = 0.95$, $c = 1.05$); and (d) +5% L_r +5% C_r –5% L_m tolerance ($a = 1.05$, $b = 1.05$, $c = 0.95$).

will be $[2\pi\sqrt{L_r(C_{r1}+C_{r2})}]^{-1}$, which is approximately $1/\sqrt{2}$ of the original frequency with both phases.

Unfortunately, the common capacitor multiphase LLC converter cannot achieve interleaving. This is the compromise of using a coupled resonant tank. However, lacking this feature is not a big concern because using a large capacitor filter will not impact the total size and cost too much. Also the dynamic performance can hardly be a problem for LLC converters as the middle stage especially that the switching frequency is increasing in today's power supplies.

E. Comparison of Common Capacitor and Common Inductor Technology

Common inductor technology has superior current-sharing performance throughout the entire load range. Even with the impact of the leakage inductor from the transformer, the common inductor two-phase LLC converter was able to achieve 2% current-sharing error from 20% to full load. As comparison, the current-sharing performance of common capacitor technology is less eye-catching, but still more than satisfying for most of the applications with current-sharing requirement.

In certain applications, if size is emphasized, then the common capacitor technology will be more appealing, because the

TABLE II
PARAMETERS OF THE TWO-PHASE LLC CONVERTER IN PSIM

	Resonant Inductor L_r	Resonant capacitor C_r	Magnetizing inductor L_m
Phase 1 (reference)	29 μH	12 nF	95 μH
Phase 2 (a)	30.5 μH (+5%)	12.6 nF (+5%)	100 μH (+5%)
Phase 2 (b)	28.5 μH (–5%)	12.6 nF (+5%)	100 μH (+5%)
Phase 2 (c)	30.5 μH (+5%)	11.4 nF (–5%)	100 μH (+5%)
Phase 2 (d)	30.5 μH (+5%)	12.6 nF (+5%)	90 μH (–5%)

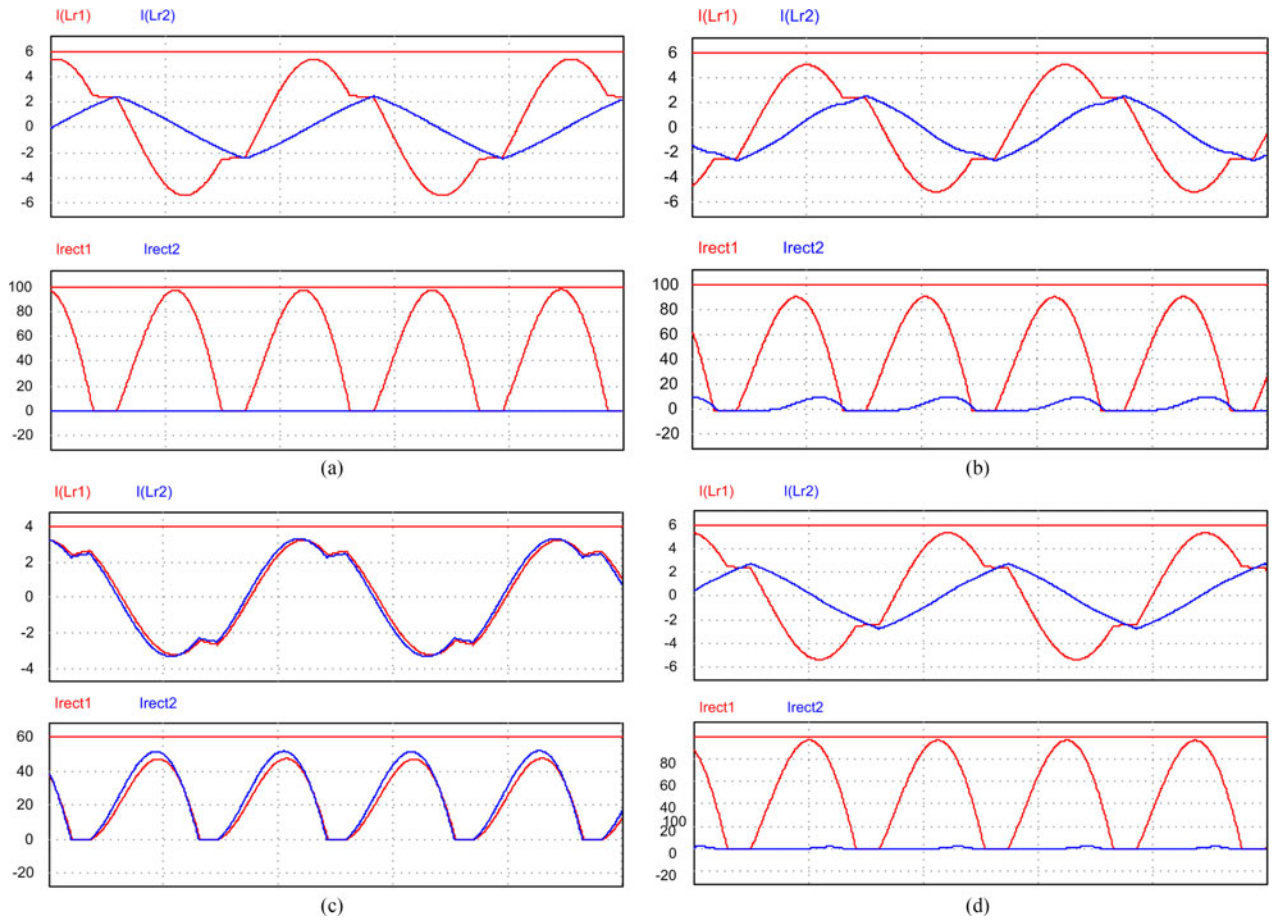

Fig. 15. PSIM simulation results of the conventional two-phase LLC converter with 5% tolerance: (a) +5% L_r +5% C_r +5% L_m tolerance ($a = 1.05$, $b = 1.05$, $c = 1.05$); (b) –5% L_r +5% C_r +5% L_m tolerance ($a = 0.95$, $b = 1.05$, $c = 1.05$); (c) +5% L_r –5% C_r +5% L_m tolerance ($a = 1.05$, $b = 0.95$, $c = 1.05$); and (d) +5% L_r +5% C_r –5% L_m tolerance ($a = 1.05$, $b = 1.05$, $c = 0.95$).

TABLE III
DATA COMPARISON OF SIMULATION AND FHA CALCULATION OF THE CONVENTIONAL TWO-PHASE LLC CONVERTER

Tolerances	FHA calculation			PSIM simulation		
	$I_{\text{rect1\_ave}}$	$I_{\text{rect2\_ave}}$	$\sigma_{\text{load\_FHA}}$	$I_{\text{rect1\_ave}}$	$I_{\text{rect2\_ave}}$	$\sigma_{\text{load\_PSIM}}$
Type a ($a = 1.05$, $b = 1.05$, $c = 1.05$)	41 A	9 A	65%	50 A	0	100%
Type b ($a = 0.95$, $b = 1.05$, $c = 1.05$)	31 A	19 A	24%	46.5 A	3.5 A	86%
Type c ($a = 1.05$, $b = 0.95$, $c = 1.05$)	24.5 A	25.5 A	2%	24 A	26 A	4%
Type d ($a = 1.05$, $b = 1.05$, $c = 0.95$)	35 A	15 A	40%	49.5 A	0.5 A	99%

resonant inductor can be integrated in the transformer core. Besides, the capacitors are easier to parallel or combine in practice. In addition, it is expected the common capacitor structure to achieve better current-sharing performance for the LCC converter. It should be noted that both technologies are very simple in structure, easy to implement, and cost effective as compared to the existing current-sharing methods.

IV. SIMULATION RESULTS

FHA is widely used as a qualitative method in the resonant converter analysis for general characteristic identification. Furthermore, to verify and compare the current-sharing performance, in this section, PSIM simulation results of both the conventional two-phase LLC converter and the proposed common capacitor LLC converter will be provided.

In Sections IV-A and IV-B, PSIM simulation results will be compared to FHA calculation for both the conventional structure and the proposed common capacitor structure at ±5% tolerances level. Four types of tolerance combinations will be included:

1) +5% L_r, +5% C_r, +5% L_m tolerance ($a = 1.05$, $b = 1.05$, $c = 1.05$);
2) –5% L_r, +5% C_r, +5% L_m tolerance ($a = 0.95$, $b = 1.05$, $c = 1.05$);

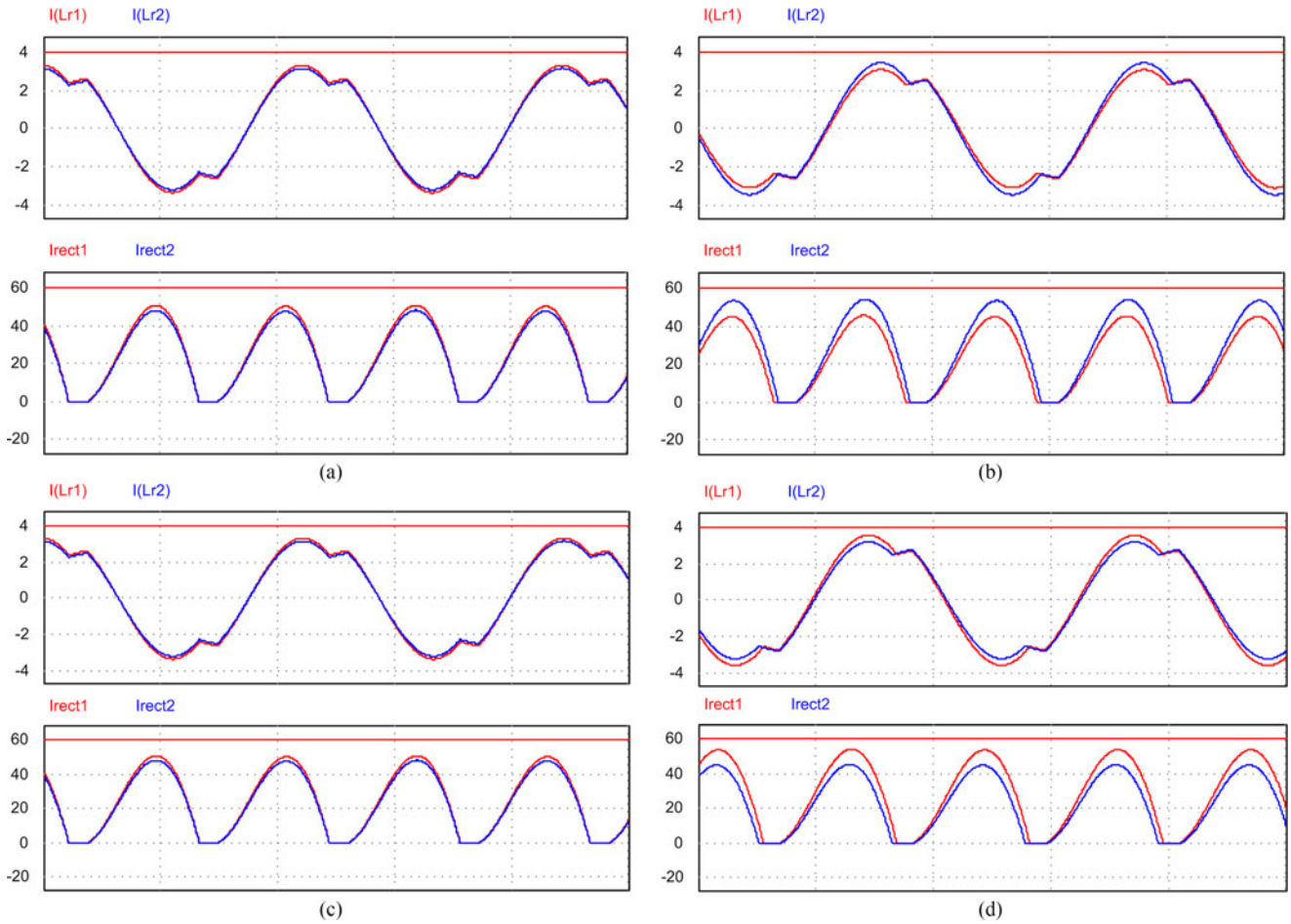

Fig. 16. PSIM simulation results of the conventional two-phase LLC converter with 5% tolerance: (a) +5% L_r +5% C_r +5% L_m tolerance ($a = 1.05$, $b = 1.05$, $c = 1.05$); (b) –5% L_r +5% C_r +5% L_m tolerance ($a = 0.95$, $b = 1.05$, $c = 1.05$); (c) +5% L_r –5% C_r +5% L_m tolerance ($a = 1.05$, $b = 0.95$, $c = 1.05$); and (d) +5% L_r +5% C_r –5% L_m tolerance ($a = 1.05$, $b = 1.05$, $c = 0.95$).

3) +5% L_r, –5% C_r, +5% L_m tolerance ($a = 1.05$, $b = 0.95$, $c = 1.05$);
4) +5% L_r, +5% C_r, –5% L_m tolerance ($a = 1.05$, $b = 1.05$, $c = 0.95$).

In Section IV-C, simulation waveforms based on the measured prototype parameters will be shown at different loads.

A. Simulation Results Under Different Tolerance

The simulation is conducted under 400 V input and total 50 A load condition. The rated output voltage is 12 V. The parameter (and tolerance percentage) is shown in Table II.

Fig. 15 shows the PSIM simulation waveforms of resonant current, rectifier current of the conventional two-phase LLC converter.

Table III shows the load current (the average value of the rectifier current $I_{\mathrm{rect1\_ave}}$ and $I_{\mathrm{rect2\_ave}}$) of FHA calculation and PSIM simulation. It can be observed that load current sharing error σ_{load} from simulation matches with the calculation results in general trends (the value is different). This is generally caused by the absence of high-order harmonics in FHA. In PSIM simulation, the worst case ($a = 1.05$, $b = 1.05$, $c = 1.05$) of load current sharing error σ_{load} reaches 100%, which means that only phase #1 provides the total 50 A load current.

Fig. 16 shows the PSIM simulation waveforms of resonant current and rectifier current of the two-phase common capacitor LLC converter. In Fig. 16(a) and (c) when the tolerance on L_r and the tolerance on L_m deviate in the same direction, the two-phase current is almost identical, which verifies the FHA calculation results in Fig. 14(a) and (c). Also, good current sharing could be achieved when the tolerance on L_r and the tolerance on L_m deviate in the opposite direction shown in Fig. 16(b) and (d).

Table IV shows the load current data comparison of FHA calculation and PSIM simulation for the common capacitor two-phase LLC converter. The results match well in trends, while have some discrepancy. At worst case ($a = 1.05$, $b = 1.05$, $c = 0.95$), in PSIM simulation, the load current difference between the two phases (σ_{load}) is only 12%.

B. Error of FHA Analysis and PSIM Simulation

It is noted that computer simulation result by PSIM is more accurate than the FHA analysis. From Table III, it is observed that for the conventional two-phase LLC converter, the PSIM

TABLE IV
DATA COMPARISON OF SIMULATION AND FHA CALCULATION OF THE COMMON CAPACITOR LLC CONVERTER

Tolerances	FHA calculation			PSIM simulation		
	$I_{\mathrm{rect1\_ave}}$	$I_{\mathrm{rect2\_ave}}$	$\sigma_{\mathrm{load\_FHA}}$	$I_{\mathrm{rect1\_ave}}$	$I_{\mathrm{rect2\_ave}}$	$\sigma_{\mathrm{load\_PSIM}}$
Type a ($a = 1.05, b = 1.05, c = 1.05$)	25.5 A	24.5 A	2%	25.5 A	24.5 A	2%
Type b ($a = 0.95, b = 1.05, c = 1.05$)	17 A	33 A	36%	23 A	27 A	8%
Type c ($a = 1.05, b = 0.95, c = 1.05$)	25.5 A	24.5 A	2%	25.5 A	24.5 A	2%
Type d ($a = 1.05, b = 1.05, c = 0.95$)	34 A	16 A	37%	28 A	22 A	12%

TABLE V
EXPERIMENTAL PROTOTYPE PARAMETERS

	Resonant Inductor L_r	Resonant capacitor C_r	Magnetizing inductor L_m
Phase 1	28.5 μH	12 nF	92 μH
Phase 2	31 μH (+8.9%)	13 nF (+8.3%)	95 μH (+3.2%)

simulation results are generally worse than the FHA calculation results. While in Table IV, the PSIM simulation result (the accurate result) is better. The difference between PSIM simulation and FHA calculation is that in the FHA method, the higher order harmonics in the resonant tank are neglected. At given load current and input voltage condition, the voltage gain calculated by FHA is lower than the actual case since only the fundamental harmonic is considered. Thus, in order to achieve the same output voltage, the switching frequency predicted by the FHA method will be lower than the actual switching frequency predicted by PSIM simulation.

From Fig. 7, the conclusion is at higher frequency, the current-sharing error is larger. Thus, for the conventional structure, in PSIM simulation, the current-sharing performance is worse than the FHA prediction.

On the contrary, for the common capacitor LLC converter, the current-sharing error is reduced with the increase in switching frequency, as shown in Fig. 12. Then, the PSIM results are better than the FHA prediction.

C. Simulation Results for the Parameters Used in Experimental Prototype

The parameters and tolerances based on experimental prototype are shown in Table V. The designed total power is 600 W (300 W$*$2).

Fig. 17 shows the simulation waveforms of conventional and proposed two-phase LLC resonant converters when the total load current is 15, 25, and 50 A. Common capacitor two-phase LLC converter could achieve significantly improved load current sharing.

Table VI shows the resonant current sharing error $\sigma_{\mathrm{resonant}}$ and load current sharing error σ_{load} based on the prototype parameters and tolerances of both the conventional two-phase LLC converter and the common capacitor two-phase LLC converter under 15, 25, and 50 A.

In Table VI, it is observed that resonant current sharing error is generally lower than load current sharing error due to the existence of the circulating current in the primary side. However, at heavy load, when the resonant current sharing error is low, the load current sharing error becomes very reasonable. Thus, it is believed that good resonant current sharing guarantees good load current sharing at heavy load.

D. Simulation Results for the Parameters Used in Other Papers

To strengthen the conclusion, resonant parameter design from [40] and [41] is simulated. The results lead to the same conclusion. The specification of the design for the two phases is shown in Table VII. Phase #1 design is the same as that in [38] and [39]. Phase #2 design has $+5\%$ on L_r, $+5\%$ on C_r, –5% on L_m, which is the worst case.

The simulations are conducted at full load condition (600 W for each phase) and two input voltage levels including 350 V (below resonance) and 400 V (above resonance). Fig. 18 shows the waveforms of the resonant current and rectifier current at 350 and 400 V. It is observed that the two phases' current is very close in magnitude, no matter the operation is below or above resonance.

Table VIII summarizes the current-sharing error, which justifies quite good current-sharing performance with 2.5–4.3% sharing error. Thus, it could be concluded that the proposed the common capacitor method is universally valid for LLC converters.

V. EXPERIMENTAL RESULTS

A 600 W two-phase LLC converter prototype using common capacitor current sharing technology is built to verify the feasibility and to demonstrate the advantages of the proposed method. The circuit diagram is shown in Fig. 10. The resonant tank parameter is designed based on the existing design method for single-phase. The specification of the prototype is shown in Table IX. In the experiment, the current on the secondary side could be as high as 50 A, and the printed circuit board (PCB) track should be as short as possible to eliminate the impact of the parasitic inductor. Thus, it is not appropriate or easy to measure the load current of each phase directly. As mentioned above, good resonant current sharing indicates good load current sharing. Thus, resonant currents are measured for evaluation of current-sharing performance.

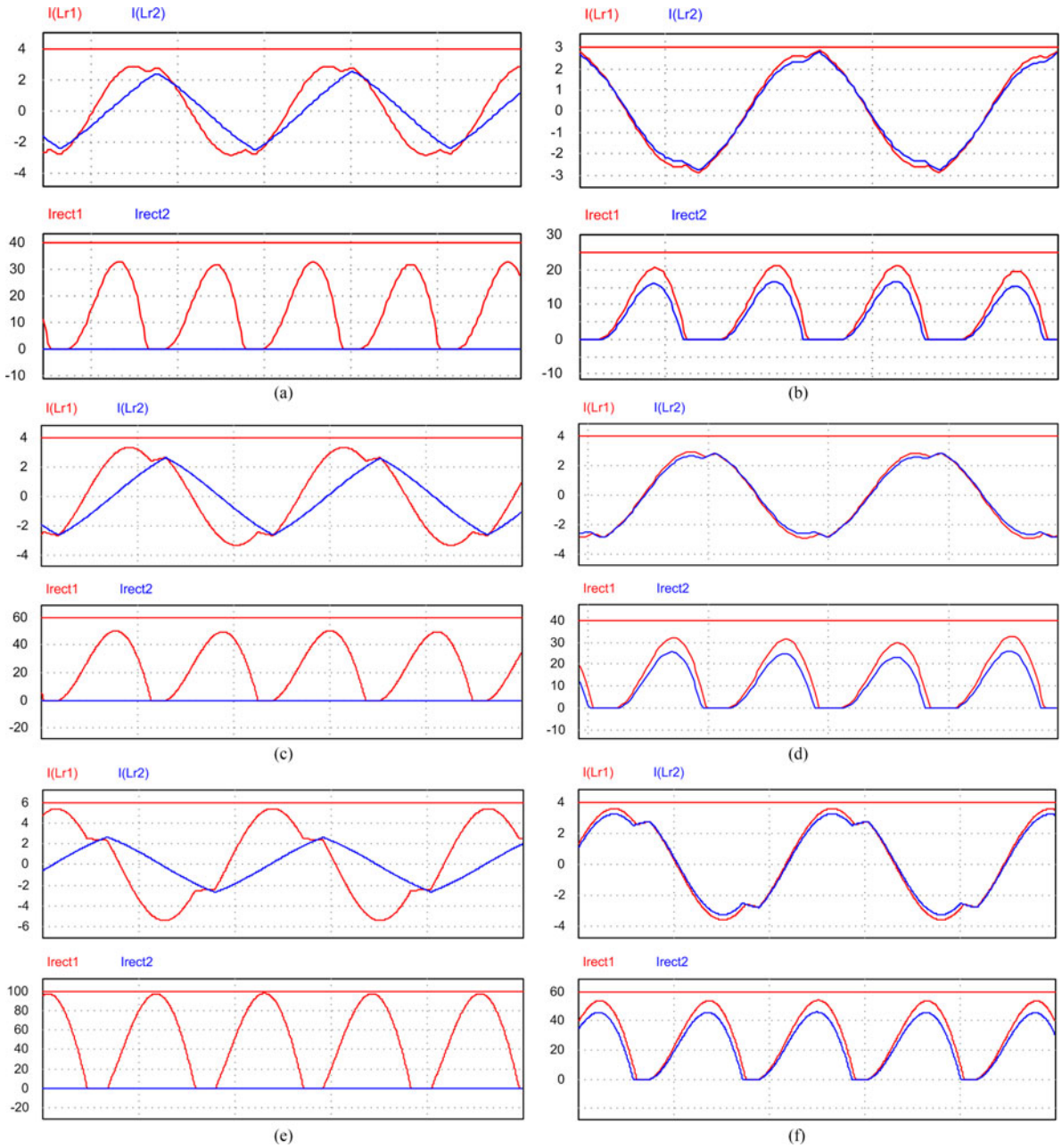

Fig. 17. PSIM simulation results of the conventional two-phase LLC converter with 5% tolerance.

TABLE VI
CURRENT-SHARING ERROR AT EXPERIMENTAL PARAMETER TOLERANCE

Total current	Phase	Conventional two-phase LLC				Common capacitor two-phase LLC			
		I_{Lr_rms}	$\sigma_{resonant}$	I_{rect_ave}	σ_{load}	I_{Lr_rms}	$\sigma_{resonant}$	I_{rect_ave}	σ_{load}
15A	Phase #1	2.1 A	16.7%	15 A	100%	2.0 A	2.6%	8.5 A	13.3%
	Phase #2	1.5 A		0 A		1.9 A		6.5 A	
25A	Phase #1	2.4 A	23.1%	25 A	100%	2.2 A	4.8%	14 A	12%
	Phase #2	1.5 A		0 A		2.0 A		11 A	
50A	Phase #1	3.7 A	42.3%	50 A	100%	2.6 A	6.1%	27.5 A	10%
	Phase #2	1.5 A		0 A		2.3 A		22.5 A	

TABLE VII
PARAMETER DESIGN FROM [40] AND [41]

Nominal input voltage	350–400 V	
Output voltage	12 V	
Full load power	600 W each phase, 1200 W total	
Transformer turns ratio	16: 1	
Resonant frequency	300 kHz	
Series inductance	#1: 10 μH	#2: 10.5 μH (+5%)
Series capacitance	#1: 27.2 nF	#2: 28.6 nF (+5%)
Magnetizing inductance	#1: 110 μH	#2: 104.5 μH (–5%)

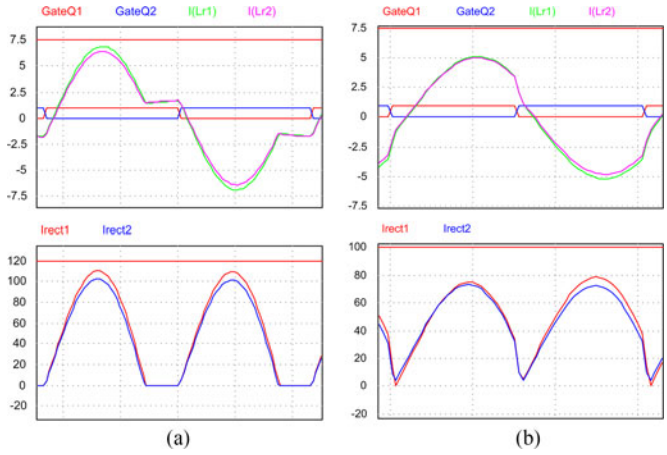

Fig. 18. Current waveform of two phases (a) 350 V and (b) 400 V.

TABLE VIII
CURRENT OF TWO PHASES AND CURRENT-SHARING ERROR (1200 W, 12 V/50 A)

	iLr1_rms	iLr1_rms	σ
350 V, 220 kHz	4.28 A	3.98 A	3.6%
400 V, 330 kHz	3.76 A	3.58 A	2.5%

TABLE IX
PROTOTYPE PARAMETERS

Switching frequency	180–270 kHz
Input voltage	350–400 V
Output voltage	12 V
Output power	300 W $\times$ 2
Transformer ratio n	20:1
Series capacitance (C_r)	12 nF (Phase1)13 nF (Phase2)
Resonant inductance (L_r)	28.5 μH (Phase1)31 μH (Phase2)
Magnetizing inductance (L_m)	92 μH (Phase1)95 μH (Phase2)
Output capacitance	1790 μF (100 μF $\times$ 8 + 330 μF $\times$ 3)
Half-bridge MOSFET	IPB60R190C6
SR MOSFET	BSC011N03LS

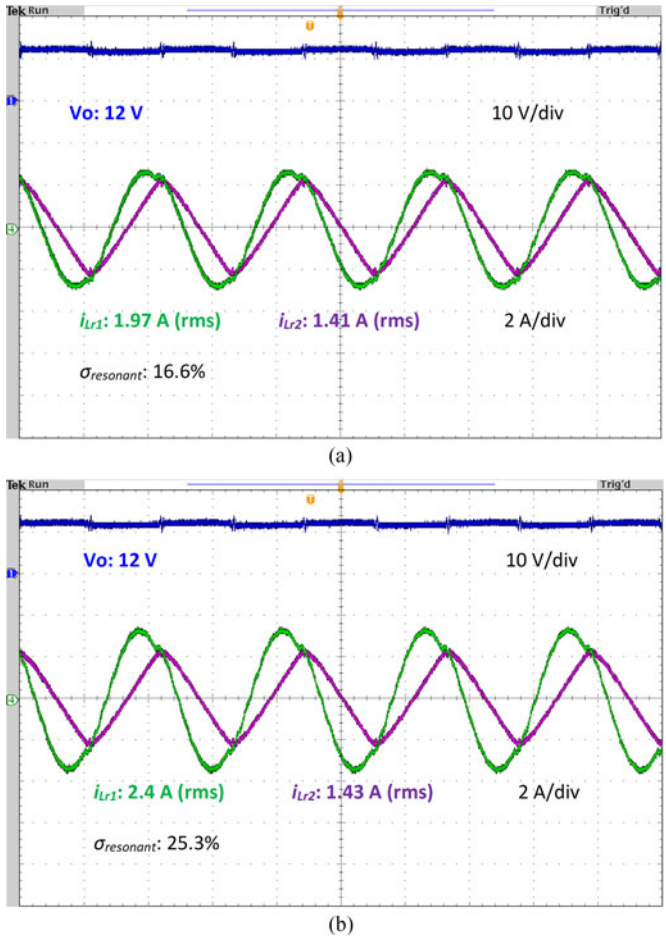

Fig. 19. Experimental waveform of the conventional two-phase LLC converter (a) 15 A load and (b) 25 A load.

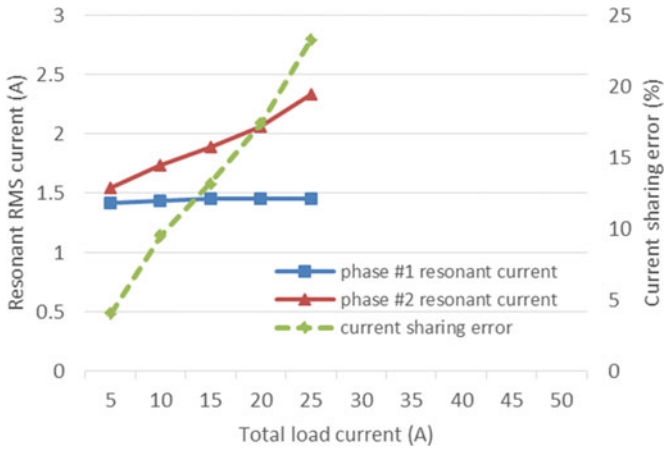

Fig. 20. Resonant current of the two-phase conventional LLC converter.

Fig. 19 shows the experiment waveform of the conventional two-phase LLC converter at 15 and 25 A total load current. Channel 1 is the output voltage. Channel 3 and channel 4 are the resonant current of two phases. As shown in Fig. 19(a) and (b), the resonant current i_{Lr2} is almost triangular waveform (basically magnetizing current for the transformer), which means phase two does not provide any load current. The prototype was designed for 25 A rated current; thus, total 50 A load test is not conducted in order to avoid any possible damage of the prototype.

Fig. 20 shows the resonant currents and the resonant current error of the conventional two-phase LLC converter at different load conditions. Resonant current of phase #2 is constant, while phase #1 current increases linearly with the increase in load

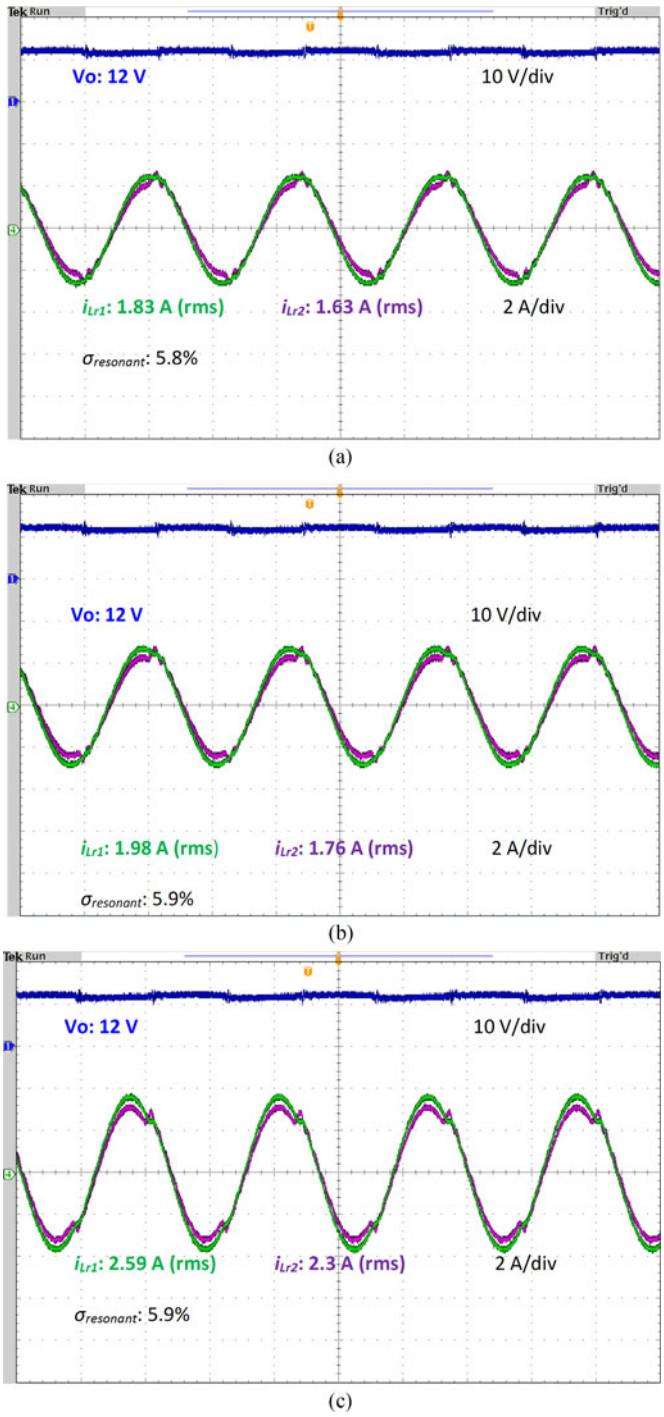

Fig. 21. Experimental waveform of the proposed common capacitor two-phase LLC converter (a) 15 A load, (b) 25 A load, and (c) 50 A load.

current. The resonant current sharing error increases from 10% to 25% when the load current changes from 5 A (60 W) to 25 A (300 W).

Fig. 21 shows the experiment waveform of the proposed common capacitor two-phase LLC converter at 15, 25, and 50 A total load current. The resonant current i_{Lr1} and i_{Lr2} are almost the same, and the resonant current error between the two phases is less than 6% for all load conditions.

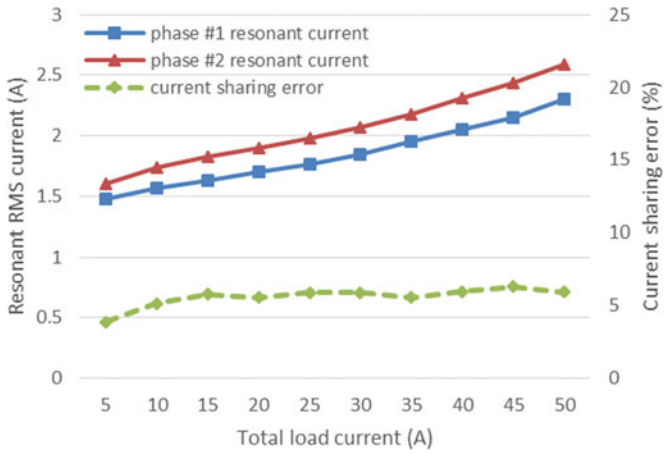

Fig. 22. Resonant current of the common capacitor two-phase LLC converter.

Fig. 22 shows the resonant currents and the resonant current error of the common capacitor two-phase LLC converter at different load conditions. When the total load current increases, the resonant currents of the two phases both increase with same slope. The resonant current error is kept under 6% for the entire load range. Compared with the conventional two-phase LLC converter, resonant current sharing error is significantly reduced.

VI. Conclusion

This paper proposed a new structure for the multiphase LLC resonant converter using a common capacitor to achieve load current sharing. The series resonant capacitors in each LLC phase are connected in parallel. The proposed common capacitor multiphase LLC converter achieves current sharing with no extra component or control. To verify the current-sharing performance, a new mathematical model is built based on the FHA method. The model can be used to analyze the current-sharing characteristics of both the conventional multiphase and the proposed common capacitor LLC converters (coupled resonant tank). The FHA analysis is compared to PSIM simulation results, and the error of the FHA method is evaluated for both the conventional two-phase LLC converter and the common capacitor LLC converter. A two-phase LLC converter prototype with 300 W per phase is built, and experiment results verify that the current-sharing error is significantly reduced with the proposed common capacitor method.

References

[1] B. Yang, "Topology investigation for front end dc/dc power conversion for distributed power system," Ph.D. dissertation, Virginia Polytech. Inst. State Univ., Blacksburg, VA, USA, 2003.

[2] Y. Zhang, D. Xu, M. Chen, Y. Han, and Z. Du, "LLC resonant converter for 48 V to 0.9 V VRM," in *Proc. 2004 IEEE 35th Annu. Power Electron. Spec. Conf.*, vol. 3, 2004, pp. 1848–1854.

[3] B. Yang, F. C. Lee, A. J. Zhang, and H. Guisong, "LLC resonant converter for front end dc/dc conversion," in *Proc. 17th Annu. IEEE Appl. Power Electron. Conf. Expo.*, vol. 2, 2002, pp. 1108–1112.

[4] I. Batarseh, "Resonant converter topologies with three and four energy storage elements," *IEEE Trans. Power Electron.*, vol. 9, no. 1, pp. 64–73, Jan. 1994.

[5] R. Severns, "Topologies for three element resonant converters," in *Proc. 5th Annu. Appl. Power Electron. Conf. Expo.*, 1990, pp. 712–722.
[6] R. P. Severns, "Topologies for three-element resonant converters," *IEEE Trans. Power Electron.*, vol. 7, no. 1, pp. 89–98, Jan. 1992.
[7] T. B. Soeiro, J. Muhlethaler, J. Linner, P. Ranstad, and J. W. Kolar, "Automated design of a high-power high-frequency LCC resonant converter for electrostatic precipitators," *IEEE Trans. Ind. Electron.*, vol. 60, no. 11, pp. 4805–4819, Nov. 2013.
[8] L. Zhe, P. Chun-Yoon, K. Jung-Min, and K. Bong-Hwan, "High-power-factor single-stage LCC resonant inverter for liquid crystal display backlight," *IEEE Trans. Ind. Electron.*, vol. 58, no. 3, pp. 1008–1015, Mar. 2011.
[9] M. C. Tsai, "Analysis and implementation of a full-bridge constant-frequency LCC-type parallel resonant converter," *IEE Proc. Electr. Power Appl.*, vol. 141, pp. 121–128, 1994.
[10] I. Batarseh, R. Liu, C. Q. Lee, and A. K. Upadhyay, "Theoretical and experimental studies of the LCC-type parallel resonant converter," *IEEE Trans. Power Electron.*, vol. 5, no. 2, pp. 140–150, Apr. 1990.
[11] X. Qu, S.-C. Wong, and C. K. Tse, "An improved LCLC current-source-output multistring LED driver with capacitive current balancing," *IEEE Trans. Power Electron.*, vol. 30, no. 10, pp. 5783–5791, Oct. 2015.
[12] N. Shafiei, M. Pahlevaninezhad, H. Farzanehfard, and S. R. Motahari, "Analysis and implementation of a fixed-frequency LCLC resonant converter with capacitive output filter," *IEEE Trans. Ind. Electron.*, vol. 58, no. 10, pp. 4773–4782, Oct. 2011.
[13] C. M. Bingham, A. Yong Ann, M. P. Foster, and D. A. Stone, "Analysis and control of dual-output LCLC resonant converters with significant leakage inductance," *IEEE Trans. Power Electron.*, vol. 23, no. 4, pp. 1724–1732, Jul. 2008.
[14] H. M. Suryawanshi and S. G. Tarnekar, "Modified LCLC-type series resonant converter with improved performance," *IEE Proc. Electr. Power Appl.*, vol. 143, pp. 354–360, 1996.
[15] Y. Chen, H. Wang, Z. Hu, Y.-F. Liu, J. Afsharian, and Z. A. Yang, "LCLC resonant converter for hold up mode operation," in *Proc. 2015 IEEE Energy Convers. Congr. Expo.*, 2015, pp. 556–562.
[16] M. T. Zhang, M. M. Jovanovic, and F. C. Y. Lee, "Analysis and evaluation of interleaving techniques in forward converters," *IEEE Trans. Power Electron.*, vol. 13, no. 4, pp. 690–698, Jul. 1998.
[17] M. T. Zhang, M. M. Jovanovic, and F. C. Lee, "Analysis, design, and evaluation of forward converter with distributed magnetics-interleaving and transformer paralleling," in *Proc. 10th Annu. Appl. Power Electron. Conf. Expo.*, vol. 1, 1995, pp. 315–321.
[18] R. Hermann, S. Bernet, S. Yongsug, and P. K. Steimer, "Parallel connection of integrated gate commutated thyristors (IGCTs) and diodes," *IEEE Trans. Power Electron.*, vol. 24, no. 9, pp. 2159–2170, Sep. 2009.
[19] J. Rabkowski, D. Peftitsis, and H. P. Nee, "Parallel-operation of discrete SiC BJTs in a 6-kW/250-kHz dc/dc boost converter," *IEEE Trans. Power Electron.*, vol. 29, no. 5, pp. 2482–2491, May 2014.
[20] Z. Hu, Y. Qiu, Y.-F. Liu, and P. C. Sen, "An interleaving and load sharing method for multiphase LLC converters," in *2013 28th Annu. IEEE Appl. Power Electron. Conf. Expo.*, 2013, pp. 1421–1428.
[21] H. Figge, T. Grote, N. Froehleke, J. Boecker, and P. Ide, "Paralleling of LLC resonant converters using frequency controlled current balancing," in *Proc. IEEE Power Electron. Spec. Conf.*, 2008, pp. 1080–1085.
[22] K. Bong-Chul, P. Ki-Bum, and M. Gun-Woo, "Analysis and design of two-phase interleaved LLC resonant converter considering load sharing," in *Proc. IEEE Energy Convers. Congr. Expo.*, 2009, pp. 1141–1144.
[23] Z. Hu, Y. Qiu, L. Wang, and Y.-F. Liu, "An interleaved LLC resonant converter operating at constant switching frequency," in *Proc. 2012 IEEE Energy Convers. Congr. Expo.*, 2012, pp. 3541–3548.
[24] Z. Hu, Y. Qiu, L. Wang, and Y.-F. Liu, "An interleaved LLC resonant converter operating at constant switching frequency," *IEEE Trans. Power Electron.*, vol. 29, no. 6, pp. 2931–2943, Jun. 2014.
[25] Z. Hu, Y. Qiu, Y.-F. Liu, and P. C. Sen, "A control strategy and design method for interleaved LLC converters operating at variable switching frequency," *IEEE Trans. Power Electron.*, vol. 29, no. 8, pp. 4426–4437, Aug. 2014.
[26] E. Orietti, P. Mattavelli, G. Spiazzi, C. Adragna, and G. Gattavari, "Two-phase interleaved LLC resonant converter with current-controlled inductor," in *Proc. Power Electron. Conf.*, 2009, pp. 298–304.
[27] B.-C. Kim, K.-B. Park, C.-E. Kim, and G.-W. Moon, "Load sharing characteristic of two-phase interleaved LLC resonant converter with parallel and series input structure," in *Proc. 2009 IEEE Energy Convers. Congr. Expo.*, 2009, pp. 750–753.
[28] F. Jin, F. Liu, X. Ruan, and X. Meng, "Multi-phase multi-level LLC resonant converter with low voltage stress on the primary-side switches," in *2014 IEEE Energy Convers. Congr. Expo.*, 2014, pp. 4704–4710.
[29] E. Orietti, P. Mattavelli, G. Spiazzi, C. Adragna, and G. Gattavari, "Analysis of multi-phase LLC resonant converters," in *Proc. Power Electron. Conf.*, 2009, pp. 464–471.
[30] E. Orietti, P. Mattavelli, G. Spiazzi, C. Adragna, and G. Gattavari, "Current sharing in three-phase LLC interleaved resonant converter," in *Proc. 2009 IEEE Energy Convers. Congr. Expo.*, 2009, pp. 1145–1152.
[31] H. Wang, Y. Chen, Y.-F. Liu, J. Afsharian, and A. Z. Yang, "A common inductor multi-phase LLC resonant converter," in *Proc. 2015 IEEE Energy Convers. Congr. Expo.*, 2015, pp. 548–555.
[32] H. Wang, Y. Chen, Y. F. Liu, J. Afsharian, and Z. Yang, "A passive current sharing method with common inductor multi-phase LLC resonant converter," *IEEE Trans. Power Electron.*, vol. PP, no. 99, 2017.
[33] H. Wang *et al.*, "A common capacitor multi-phase LLC resonant converter," in *Proc. 2016 IEEE Appl. Power Electron. Conf. Expo.*, 2016, pp. 2320–2327.
[34] B. C. Kim, K. B. Park, C. E. Kim, and G. W. Moon, "Load sharing characteristic of two-phase interleaved LLC resonant converter with parallel and series input structure," in *Proc. 2009 IEEE Energy Convers. Congr. Expo.*, 2009, pp. 750–753.
[35] Y. Gang, P. Dubus, and D. Sadarnac, "Analysis of the load sharing characteristics of the series-parallel connected interleaved LLC resonant converter," in *Proc. 2012 13th Int. Conf. Optim. Electr. Electron. Equip.*, 2012, pp. 798–805.
[36] H. Wang *et al.*, "An algorithm to analyze circulating current for multi-phase resonant converter," in *2016 IEEE Appl. Power Electron. Conf. Expo.*, 2016, pp. 899–906.
[37] I. O. Lee and G. W. Moon, "The k-Q analysis for an LLC series resonant converter," *IEEE Trans. Power Electron.*, vol. 29, no. 1, pp. 13–16, Jan. 2014.
[38] H. Wang, Y. Chen, and Y. F. Liu, "A passive-impedance-matching concept for multiphase resonant converter," in *Proc. 2016 IEEE Appl. Power Electron. Conf. Expo.*, 2016, pp. 2304–2311.
[39] H. Wang, Y. Chen, and Y. F. Liu, "A passive-impedance-matching technology to achieve automatic current sharing for multi-phase resonant converter," *IEEE Trans. Power Electron.*, vol. PP, no. 99, 2017.
[40] Z. Hu, L. Wang, H. Wang, Y. F. Liu, and P. C. Sen, "An accurate design algorithm for LLC resonant converters; Part I," *IEEE Trans. Power Electron.*, vol. 31, no. 8, pp. 5435–5447, Aug. 2016.
[41] Z. Hu, L. Wang, Y. Qiu, Y. F. Liu, and P. C. Sen, "An accurate design algorithm for LLC resonant converters; Part II," *IEEE Trans. Power Electron.*, vol. 31, no. 8, pp. 5448–5460, Aug. 2016.

Hongliang Wang (M'12–SM'15) received the B.Sc. degree in electrical engineering from the Anhui University of Science and Technology, Huainan, China, in 2004, and the Ph.D. degree in electrical engineering from the Huazhong University of Science and Technology, Wuhan, China, in 2011.

From 2004 to 2005, he worked as an Electrical Engineer in Zhejiang Hengdian Thermal Power Plant. From 2011 to 2013, he worked as a Senior System Engineer in Sungrow Power Supply Co., Ltd. He has been a Post-Doctoral Fellow with Queen's University, Kingston, ON, Canada, since 2013. He has published more than 50 papers in conferences and journals. He is the Inventor/Co-inventor of 41 China issued patents, 15 US patents, and 6 PCT patents pending. His research interests include power electronics, including digital control, modulation, and multilevel topology of inverter for photovoltaic application and microgrids application; resonant converters and server power supplies, and LED drivers.

Dr. Wang is currently a senior member of China Electro-Technical Society; a senior member of China Power Supply Society (CPSS). He serves as a member of CPSS Technical Committee on Standardization; a member of CPSS Technical Committee on Renewable Energy Power Conversion; a Vice-Chair of Kingston Section, IEEE; a Session Chair of ECCE 2015; a TPC member of ICEMS 2012; and a China Expert Group Member of IEC standard TC8/PT 62786.

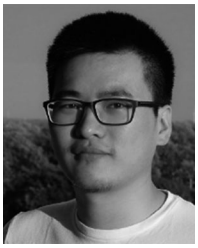

Yang Chen (S'14) received the B.Sc. and M.Sc. degrees in electrical engineering from the Beijing Institute of Technology, Beijing, China, in 2011 and 2013, respectively. He is currently working toward the Ph.D. degree with Queen's University, Kingston, ON, Canada.

His research interests include topology, control, and design of resonant converters in ac–dc and dc–dc fields, power factor correction technology, and digital control.

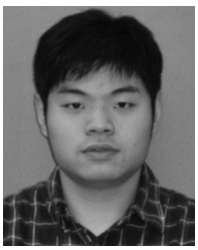

Yajie Qiu (S'13) received the M.Sc. degree from Anhui University of Technology, Anhui Sheng, China, in 2011. He received the Ph.D. degree from Queen's University, Kingston, ON, Canada, in 2017, both in electrical engineering.

He will be working as an Application Engineer in GaN Systems, Inc., from March, 2017. His research interests include topologies and control methods for ac–dc converters with power factor correction and LED driver, nonlinear control to achieve fast dynamic performance for dc–dc converters, and modulation schemes for resonant converter. He has two international patents pending.

Dr. Qiu received the outstanding presentation award at APEC'15 and a conference travel award from PSMA.

Peng Fang (S'11) received the M.Sc. degree from Hong Kong University of Science and Technology, Clear Water Bay, Hong Kong, in 2007, and the Ph.D. degree from Queen's University, Kingston, ON, Canada, in 2016, both in electrical engineering.

He continued his research in the same lab as a Postdoctoral Research Fellow. From 2008 to 2011, he worked as an R&D Power Electronics Engineer at ASM Pacific Technology, where he lead the innovation and development on switching mode power supply, switching and linear power amplifier. He has two U.S. patents pending and several inventions. His research interests include dc–dc converter design, switching capacitor converter design, offline LED driving, GaN-FET based converter design, and microinverter design.

Yan Zhang (S'09–M'14) received the B.S. and M.S. degrees from Xi'an University of Technology, Xi'an, China, in 2006 and 2009, respectively, and the Ph.D. degree from Xi'an Jiaotong University (XJTU), Xi'an, China, in 2014, all in electrical engineering.

In 2014, he then joined the Electrical Engineering School, XJTU, as a teaching faculty. Since early 2016, he is also a Postdoctoral Research Fellow in the Department of Electrical and Computer Engineering, Queen's University, Kingston, ON, Canada. His research interests include topology, model and control of power electronic systems, high step-up dc–dc converters, and power-electronics applications in renewable energy and distributed generation.

Laili Wang (S'07–M'13–SM'15) was born in Shaanxi province, China, in 1982. He received the B.S., M.S., and Ph.D. degrees in electrical engineering from Xi'an Jiaotong University, Xi'an, China, in 2004, 2007, and 2011, respectively.

In 2011, he became a Postdoctoral Fellow in the Department of Electrical Engineering, Queen's University, Kingston, ON, Canada. In 2013, he started to work as a Research Fellow in Queen's University. Since 2014, he has worked in the research center of Sumida LTD, Canada. His research focuses on package and integration of high-frequency high-power density dc/dc converters.

Yan-Fei Liu (M'94–SM'97–F'13) received the bachelor's and master's degrees in electrical engineering from the Department of Electrical Engineering, Zhejiang University, Hangzhou, China, in 1984 and 1987, respectively, and the Ph.D. degree in electrical engineering from the Department of Electrical and Computer Engineering, Queen's University, Kingston, ON, Canada, in 1994.

He was a Technical Advisor with the Advanced Power System Division, Nortel Networks, Ottawa, Canada, from 1994 to 1999. Since 1999, he has been with Queen's University, where he is currently a Professor with the Department of Electrical and Computer Engineering. He has authored more than 200 technical papers in the IEEE Transactions and conferences, and holds 20 US patents. He is also a Principal Contributor for two IEEE standards. His current research interests include digital control technologies for high efficiency, fast dynamic response dc–dc switching converter and ac–dc converter with power factor correction, resonant converters and server power supplies, and LED drivers.

Dr. Liu serves as an Editor for the IEEE JOURNAL OF EMERGING AND SELECTED TOPICS OF POWER ELECTRONICS (IEEE JESTPE) since 2013, an Associate Editor for the IEEE TRANSACTIONS ON POWER ELECTRONICS since 2001, and a Guest Editor-in-Chief for the special issue of Power Supply on Chip of the IEEE TRANSACTIONS ON POWER ELECTRONICS from 2011 to 2013. He also served as a Guest Editor for special issues of JESTPE: Miniaturization of Power Electronics Systems in 2014 and Green Power Supplies in 2016. He serves as the Co-General Chair of ECCE 2015 held in Montreal, Canada, in September 2015. He will be the General Chair of ECCE 2019 to be held in Baltimore, USA. He has been the Chair of PELS Technical Committee on Control and Modeling Core Technologies since 2013 and the Chair of PELS Technical Committee on Power Conversion Systems and Components from 2009 to 2012. He received the Award of Excellence in Technology in Nortel in 1997 and the Premier's Research Excellence Award in 2000 in Ontario, Canada.

Jahangir Afsharian received the B.S. and M.S. degrees in electrical engineering, in 2006 and 2009, respectively, from Ryerson University, Toronto, ON, Canada, where he is currently working toward the Ph.D. degree.

From 2009 to 2011, he was a Research and Development (R&D) Engineer in the Communications and Power Industries, Georgetown, ON, Canada, where he was involved in the design of resonant converter LCC and high-voltage transformer for x-ray medical equipment. From the end of 2011 to present, he is a Senior Electrical Engineer in the Advanced Development Group, Murata Power Solution, Mansfield, MA, USA, where he is involved in the power electronics ac–dc power-factor-correction and dc–dc converter. His current research interests include three-phase matrix based rectifier for battery charger and data center applications.

Zhihua (Alex) Yang was born in Hubei, China. He received the B.S. degree from Hubei Institute of Technology, Hubei, China, in 1993, and the M.S. degree from Queen's University, Kingston, ON, Canada, in 2005, both in electrical engineering.

He worked as a Design Engineer with Wuhan Zhouji Telecom Power Supply Corporation from 1993 to 2002. He has been a design engineer with the Advanced Research center, Paradigm Electronics, Inc., Canada, during 2005–2007. He joined Murata Power Solutions, Inc., Markham, ON, Canada, in 2007. Since then, he has been working as a Design Engineer, Senior Design Engineer, and Principal Design Engineer. He is currently the Director of product development in Murata Power Solutions, Inc. His research interests include high switching frequency, high power density, and high-efficiency switching mode power suppliers.